Calcium Borohydride Ca(BH$_4$)$_2$: Fundamentals, Prediction and Probing for High-Capacity Energy Storage Applications, Organic Synthesis and Catalysis

Cezar Comanescu

National Institute of Materials Physics, Atomistilor 405A, 077125 Magurele, Romania; cezar.comanescu@infim.ro

Abstract: Calcium borohydride (Ca(BH$_4$)$_2$) is a complex hydride that has been less investigated compared to its lighter counterpart, magnesium borohydride. While offering slightly lower hydrogen storage capacity (11.5 wt% theoretical maximum, 9.6 wt% under actual dehydrogenation conditions), there are many improvement avenues for maximizing the reversible hydrogen storage that have been explored recently, from DFT calculations and polymorph investigations to reactive hydride composites (RHCs) and catalytic and nanosizing effects. The stability of Ca(BH$_4$)$_2$, the possibility of regeneration from spent products, and the relatively mild dehydrogenation conditions make calcium borohydride an attractive compound for hydrogen storage purposes. The ionic conductivity enhancements brought about by the rich speciation of borohydride anions can extend the use of Ca(BH$_4$)$_2$ to battery applications, considering the abundance of Ca relative to alkali metal borohydrides typically used for this purpose. The current work aims to review the synthetic strategies, structural considerations of various polymorphs and adducts, and hydrogen storage capacity of composites based on calcium borohydrides and related complex hydrides (mixed anions, mixed cations, additives, catalysts, etc.). Additional applications related to batteries, organic and organometallic chemistry, and catalysis have been briefly described.

Keywords: calcium borohydride; hydrogen storage; thermodynamics; kinetic improvement; batteries; RHC reactive hydride composites

1. Introduction

The road to sustainable energy has an ultimate endpoint: the hydrogen economy. Hydrogen remains the only energy source producing a high amount of clean energy with no carbon-containing by-products [1–12]. However, vehicular and stationary applications relying on hydrogen technology still face major drawbacks and important technological challenges, along with safety risks associated with H$_2$ storage tanks where pressure spikes to 700 bar H$_2$ [1].

In this context, solid-state hydrogen storage represents a safer alternative to classical high pressure H$_2$ tanks, although the strict requirements of the US DOE have yet to be met [2]. The current target for 2025 is a material capable of storing 5.5 wt% hydrogen (1.8 kWh/kg, 1.3 kWh/L, with an estimated cost of $9/kWh). Perhaps the most important aspect of solid-state hydrogen storage is the material's capability to reversibly store H$_2$ without continual loss of this storage capacity. To this end, most experimental tanks have been fueled by various intermetallics (AB$_2$-type or AB$_5$-type, such as LaNi$_5$H$_6$ with 1.38 wt%), which offer a storage capacity not exceeding, at best, 2 wt% hydrogen. With a storage capacity of up to 20 wt% (Be(BH$_4$)$_2$) and high gravimetric densities (110–150 g H$_2$/L), complex hydrides are the most promising solid-state hydrogen storage materials, and the amount of research in this area has been staggering. Still, the kinetic and thermodynamic factors of absorption/desorption processes hinder their wider use, while the

potentially toxic boron-containing gases (diborane or higher homologues) are of concern for the environment.

Light metal borohydrides $M(BH_4)_n$ (M = Li, Na, Mg, Ca) and alanates have received the most attention not only for their increased theoretical hydrogen storage capacity, but also due to promising results pointing to the possibility of reversibility during successive a/d cycles. With a high storage capacity of about 10 wt% (actually attainable under experimental conditions) and a relatively low dehydrogenation temperature, $Ca(BH_4)_2$ holds promise for a viable and reversible hydrogen storage material under suitable conditions. While dehydrogenation of $Ca(BH_4)_2$ has been reported in the range 350–500 °C, this is still lower than other light metal borohydrides. Driven by the high hydrogen storage capacity of calcium borohydride needed for energy storage applications, particularly in the field of hydrogen storage and fuel cells, researchers have investigated various methods to enhance the hydrogen release kinetics and lower the dehydrogenation temperature. $Ca(BH_4)_2$ has the potential to offer high energy density, enabling the development of compact and efficient energy storage systems. Calcium borohydride can serve as both a source of energy and a hydrogen reservoir within energy storage devices, such as lithium-ion batteries and sodium-ion batteries.

However, despite its potential, there are several challenges that need to be addressed before the wide acceptance of $Ca(BH_4)_2$ as an energy storage material. The kinetics of hydrogen release from calcium borohydride are relatively slow, limiting its practical application. Enhancing hydrogen release kinetics is a key research focus. The dehydrogenation reaction mechanisms of calcium borohydride are not yet fully understood, and further investigation is required to gain detailed insights into the underlying processes. Another obstacle comes from an economic point of view. The cost of $Ca(BH_4)_2$ is high; therefore, the development of cost-effective and scalable synthesis routes for calcium borohydride is another area that requires more research results.

The current review aims to describe the most significant aspects concerning $Ca(BH_4)_2$, from the synthesis routes, crystal structure and polymorphs, structural variability and modifications (DFT computations, nanoconfinement, destabilization, RHCs, solvates/adducts), characterization methods, hydrogen storage properties, and further applications in battery technology, organic synthesis, and organometallic chemistry. Optimizing the overall performance, stability, and efficiency of energy storage devices utilizing calcium borohydride is a critical research challenge.

2. Synthesis Routes

There are various methods reported for the synthesis of borohydrides [5,13] and, in particular, of $Ca(BH_4)_2$. For instance, Barkhordarian et al. reported the hydrogenation of the RHC: CaH_2 + MgB_2 at 350 °C and 140 bar H_2 to produce $Ca(BH_4)_2$ + MgH_2 (Equation (1)) [13].

$$CaH_2 + MgB_2 + 4\,H_2 \xrightarrow{250\,°C,140\,bar\,H_2} Ca(BH_4)_2 + MgH_2 \quad \Delta H = -27.5\,kg/mol \quad (1)$$
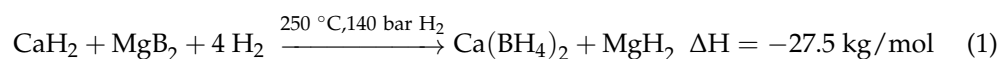
However, the layered structure of B in MgB_2 was essential for Equation (1) to occur, as no reactivity was observed when substituting MgB_2 for B. The reasoning seemed to lie in the structural features of MgB_2, where layers of B are located between layers of Mg, a structure bearing similarities to graphite. The authors also reported enhanced kinetics of de-/rehydrogenation when using $Ti(O^iPr)_4$ as an additive [13].

Dodecahydroborates have been obtained by desolvation at ~120 °C of the $MB_{12}H_{12}$ solvates, or in their pure form, by the following Equation (2) [14], The mixture of $M(BH_4)_2$ and $B_{10}H_{14}$ is typically milled in a planetary ball mill (10 steel balls, 7 mm diameter, 0.1 MPa Ar, 5 h milling), followed by sintering in stainless steel crucibles at 380 °C for 2 h in the case of $CaB_{12}H_{12}$ [14].

$$M(BH_4)_2 + B_{10}H_{14} \rightarrow MB_{12}H_{12} + 5\,H_2 \ (M = Mg,\ Ca) \qquad (2)$$
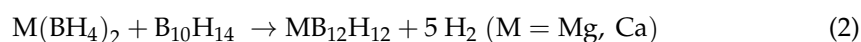
Nanostructuring has long been utilized to achieve significantly better yields for reactions where classical synthetic routes have failed [6], while stabilization of reactive species has often been attained via complex formation, i.e., through ligand coordination, as is the case for ammine solvates of $M(BH_4)_2$ (M = Ca, Sr) [15]. Jepsen et al. reported the synthesis of four such solvates in the case of calcium-based borohydrides: $Ca(NH_3)_n(BH_4)_2$ (n = 1, 2, 4, and 6) (Equation (3)) [15]. The pure $Ca(BH_4)_2$ absorbs gaseous ammonia, forming the unstable hexa-ammine calcium borohydride $Ca(NH_3)_6(BH_4)_2$, which undergoes a rapid decomposition equilibrium to form the tetra-ammine calcium borohydride $Ca(NH_3)_4(BH_4)_2$.

$$Ca(BH_4)_2 + 6\,NH_{3\,(g)} \rightarrow Ca(NH_3)_6(BH_4)_2 \leftrightarrow Ca(NH_3)_4(BH_4)_2 + 2\,NH_{3\,(g)} \tag{3}$$
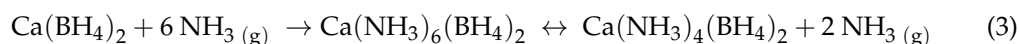
Karabulut et al. synthesized $Ca(BH_4)_2$ in a solid-state reaction starting from anhydrous, synthetic colemanite, a calcium borate mineral of formula $Ca_2B_6O_{11}.5H_2O$ [16]. By milling $Ca_2B_6O_{11}$ and CaH_2 in a 1:12 molar ratio in a spex-mill, calcium borohydride was obtained with a sole by-product in the form of CaO (Equation (4)). Using colemanite as the raw material has a clear economic advantage, as the cost of 1 g $Ca(BH_4)_2$ would be ~\$4, compared to the commercial version's (~\$200).

$$Ca_2B_6O_{11} + 12\,CaH_2 \rightarrow Ca(BH_4)_2 + 11\,CaO \tag{4}$$
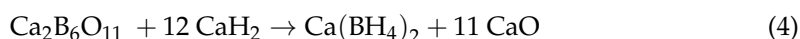
It is also interesting to note that the hydrogen content of $Ca(BH_4)_2$ could effectively double when subjected to hydrolysis, as $Ca(BO_2)_2$ is the main product along with H_2 (Equation (5)).

$$Ca(BH_4)_2 + 4\,H_2O \rightarrow Ca(BO_2)_2 + 8\,H_2 \tag{5}$$
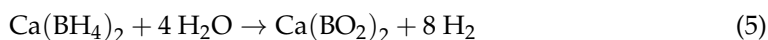
Given the reactivity of metal borohydrides towards water, it follows that the formation of a bimetallic borohydride in the form of $LiCa_3(BH_4)(BO_3)_2$, as isolated and characterized by Lee et al., is not that surprising after all [17]. The mixed borohydride was isolated from hydrogenation studies carried out on RHC based on 0.75 $LiBH_4$–0.25 $Ca(BH_4)_2$ embedded in a mesoporous carbon matrix (V_p = 1.15 cm^3/g), and most likely originates from oxygen-containing impurities (oxygen or water) [17]. The formation of $LiCa_3(BH_4)(BO_3)_2$ was tracked by XRD and was found to proceed through the intermediacy of mixed anion calcium borohydride, $Ca_3(BH_4)_3(BO_3)$ (Equation (6)).

$$LiBH_4 + 2\,Ca_3(BH_4)_3(BO_3) \rightarrow LiCa_3(BH_4)(BO_3)_2 + 3\,Ca(BH_4)_2 \tag{6}$$
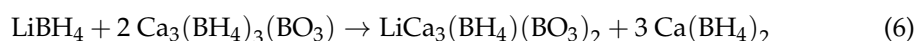
The general route to prepare $Ca(BH_4)_2$ starts from CaH_2 or alkoxide $Ca(OR)_2$ and B_2H_6, or more conveniently by wet chemistry in a metathesis reaction, where $CaCl_2$ and $NaBH_4$ are ball milled in THF (tetrahydrofuran), producing the commercially available THF adduct of calcium borohydride, namely, $Ca(BH_4)_2.2THF$ [18,19] (Equation (7)).

$$2\,NaBH_4 + CaCl_2 \xrightarrow{THF} Ca(BH_4)_2 \cdot 2THF + 2\,NaCl \tag{7}$$
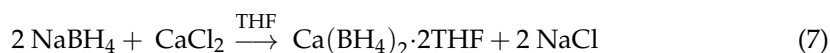
Other adducts of $Ca(BH_4)_2$ are also reported; for instance, desolvation of $Ca(BH_4)_2.2THF$ at 80 °C led to the formation of $Ca(BH_4)_2 \cdot THF$, as reported by Richter et al. [20].

Møller et al. reported the synthesis of $M(BH_4)_n$ from the systems AlB_2–MH_x (M = Li, Na, Ca, but not Mg), where AlB_2 served as a boron source, and H_2 was introduced at a pressure in the range of 100–600 bar [21] (Equation (8)).

$$AlB_2 + \frac{2}{x}MH_x + 3\,H_2 \rightarrow \frac{2}{x}\,M(BH_4)_x + Al \tag{8}$$
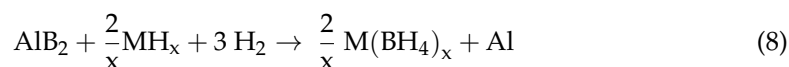
The inclusion of Al in the case of $Ca(BH_4)_2$ can produce 6.3 wt% with a reaction enthalpy of 64.9 kJ/mol H_2 and an entropy of 156.5 J/k mol H_2, requiring a temperature

of 140 °C at an equilibrium H_2 pressure of 1 bar (Equation (9)). This alone is a marked improvement compared to neat $Ca(BH_4)_2$ (87.2 kJ/mol H_2, 158.3 J/K mol H_2, 280 °C) [21].

$$Ca(BH_4)_2 + Al \leftrightarrow AlB_2 + CaH_2 + 3 H_2 \qquad (9)$$
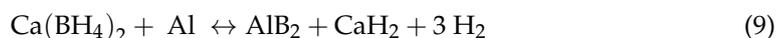
Nakagawa et al. used ball milling of CaH_2–CaB_6 mixtures to obtain $Ca(BH_4)_2$ near room temperature, noting the important role of crystalline CaB_6 in order to achieve reasonably high rates for hydrogenation [22].

Several experimental aspects have to be considered when synthesizing $Ca(BH_4)_2$, along with strong safety protocols. For instance, the influence of chlorides was illustrated in the mixture $CaCl_2$:$LiBH_4$, when the reactant ratio needs to be carefully optimized, otherwise solid solutions $Li(BH_4)_{1-x}Cl_x$/$Ca(BH_4)_{2-y}Cl_y$ (milling performed under an Ar atmosphere) are obtained, and $CaHCl$ forms instead of $Ca(BH_4)_2$ [23]. $Ca(BH_4)_2$ was also produced by milling CaB_6 with CaH_2 in a 1:2 molar ratio under 700 bar H_2 at 400–440 °C, as evidenced by Ronnebro and Majzoub [11].

$Ca(BH_4)_2$ can serve as as borohydride source for other metathesis reactions, for instance with $M_2(SO_4)_x$ metal sulfates, with the driving force for obtaining $M(BH_4)_x$ being the formation of the precipitate of $CaSO_4$ [18]. Other authors have reported a mixed adduct $Ca(BH_4)_2 \cdot Al(BH_4)_3$ resulted by mixing the unsolvated starting borohydrides, decomposing into starting borohydrides upon heating, and having a postulated structure $[Ca(BH_4)]^+[Al(BH_4)_4]^-$ supported by IR spectrum analysis [24].

3. Structural Variability, Polymorphs, Crystal Structure, DFT Predictions, and Phase Transitions

The structural stability aspects of many representative simple and complex hydrides (alanates, borohydrides) have been reviewed in the recent past [25], along with Ca-based RHCs ([$Ca(BH_4)_2$ + MgH_2 and $Ca(BH_4)_2$ + MgH_2 + $0.1NbF_5$]) [26]. Karimi et al. have highlighted the catalytic role of NbF_5 on the hydrogen sorption kinetics of $Ca(BH_4)_2$ + MgH_2 (10.5 wt% H_2), when ~10 nm diameter NbB_2 was evidenced to form and to remain stable during a/d cycles, while also being responsible for producing ~50% finer Ca-RHC + $0.1NbF_5$ nanocomposites and preventing agglomeration of calcium-RHCs [26].

The structural features of $Ca(BH_4)_2$ have been described by Llamas-Jansa et al., who reported the different behavior between α, β, and γ polymorphs of $Ca(BH_4)_2$ during hydrogenation studies [27]. Vibrational spectroscopy data was employed to correlate the increase in wavenumber to the increased decomposition temperature (15 °C between the α and γ polymorphs). The most effective H_2 release was observed when ramping at 10 °C/min a sample of pure α-$Ca(BH_4)_2$ [27]. Moreover, Sharma et al. shed light on the B-H bond breaking/formation, using isotope exchange reactions with a D_2 pressure of 20 bar, concluding an activation energy $E_a = 82.1 \pm 2.7$ kJ mol^{-1} for the transformation of $Ca(BH_4)_2$ into $Ca(BD_4)_2$, and proposing a mechanistic scheme involving the formation of an activated complex: $Ca((BH_4)_2 + D_2 \leftrightarrow$ Activated complex $\rightarrow Ca(BD_xH_{4-x})_2$ [28]. Considering all the literature data, it seems that the dehydrogenation behavior of $Ca(BH_4)_2$ depends greatly on the polymorph composition and their respective ratio in the starting sample material, especially considering the typical co-existence of α and β phases during hydrogenation experiments [29]. Soloninin et al. studied the reorientation motion of BH_4 tetrahedra in $M(BH_4)_2$ (M = Mg, Ca) by proton and ^{11}B spin-lattice relaxation rates and found that at low temperatures, the reorientation in the β phase is faster (E_a = 100–116(5) meV for β-, E_a = 286(7) meV for α-$Ca(BH_4)_2$), and depends on the changes in the local environment of BH_4 groups [29].

3.1. Crystal Structure, Polymorphs, and Phase Transitions

The two most common phases of calcium borohydride are α-$Ca(BH_4)_2$ (lattice parameters: a = 8.7782(2) Å, b = 13.129(1) Å, c = 7.4887(9) Å; 300 K) and β-$Ca(BH_4)_2$ (a = 6.9509(5) Å, c = 4.3688(3) Å, 433 K). The alpha phase is stable from 0 K to 440 K, while from 440 K, the high temperature phase, β-$Ca(BH_4)_2$ becomes dominant. The metastable

γ-Ca(BD$_4$)$_2$ crystal structure was reported by combined X-ray and neutron measurements, and was refined in the orthorhombic space group *Pbca* (a = 7.525(1) Å, b = 13.109(2) Å, c = 8.403(1) Å) [30,31]. The γ phase is less stable than the α phase, and its stability decreases with temperature; the expected phase transitions are expected to follow the trend α-Ca(BH$_4$)$_2$ → γ-Ca(BH$_4$)$_2$ → β-Ca(BH$_4$)$_2$ [30]. There have been some debates regarding the space group of both α and β phases; for instance, DFT computations conducted by Le et al. [32] over the hydrostatic pressure range 0–40 GPa showed that the *F2dd* space group seems to be the preferred structure of α-Ca(BH$_4$)$_2$ at low temperatures [32]. Crystal structures and total energy have been calculated based on the general gradient approximation (GGA) method for density functional theory (DFT), implemented by the ABINIT simulation package, while Hartwigsen–Goedecker–Hutter pseudopotentials have been used for calculations, and the exchange–correlation interactions were described by the Perdew–Burke–Ernzerhof (PBE) GGA functional [32]. The transition to the beta phase at higher temperatures was supported by calculations performed by Lee et al. [33], who pointed out a vibrational entropy excess of β-Ca(BH$_4$)$_2$ over α-Ca(BH$_4$)$_2$ of 16 J/(mol K). A total of nine possible crystal structures have been proposed in the literature for calcium borohydride: three α phases, one α' phase, four β phases, and one γ phase [34]. The most agreed-upon structures are, however, the α and β phases [35] (Table 1).

Table 1. Crystal structure of calcium borohydride with corresponding space groups, decomposition temperatures (and rehydrogenation temperatures, where available) (°C), and crystal systems.

Metal Borohydride	Decomposition Temperature (°C)	Rehydrogenation Temperature (°C)	Space Group	Crystal System	Ref.
α-Ca(BH$_4$)$_2$	347–387 °C, 397–497 °C (2-step)	RT stable	*Fddd* or *F2dd*	Orthorhombic	[32,35,36]
β-Ca(BH$_4$)$_2$	α−Ca(BH$_4$)$_2$ $\xrightarrow{167\ °C}$ β-Ca(BH$_4$)$_2$; 330–400 °C	RT, metastable, HT polymorph	P4$_2$/m or P$\bar{4}$	Tetragonal	[33,36]
α'-Ca(BH$_4$)$_2$	-	-	I$\bar{4}$2d	Tetragonal	[35]
γ-Ca(BD$_4$)$_2$	-	-	Pbca	Orthorhombic	[30,31]
CaB$_{12}$H$_{12}$	-	-	C2/c	Monoclinic	[37]

Other reports have dealt with phase variation occurring via desolvation from the adduct Ca(BH$_4$)$_2$.2THF when a mixture of α-Ca(BH$_4$)$_2$ and γ-Ca(BH$_4$)$_2$ polymorphs was observed experimentally [35]. Filinchuk et al. have also reported a second-order transition, α-Ca(BH$_4$)$_2$ (*F2dd*) → α'-Ca(BH$_4$)$_2$ (I-42d), occurring at ~495 K [35]. The various polymorphs of α-Ca(BH$_4$)$_2$ (prepared by desolvation of commercially available Ca(BH$_4$)$_2$.2THF at 433 K for 1 h) have also been investigated under high pressure (10.4 GPa, room temperature) by Liu et al. [38] by combined Raman and IR spectroscopies, and it was found that the transformations are reversible throughout the pressure region investigated [38]. The authors also pointed out the need to start the compression from phase-pure Ca(BH$_4$)$_2$, otherwise H$_2$ release and interaction in mixtures α-Ca(BH$_4$)$_2$–β-Ca(BH$_4$)$_2$ (which are the typical starting point) would further complicate the analysis of lattice, bending, and stretching modes [38]. In order to avoid the α-Ca(BH$_4$)$_2$ → β-Ca(BH$_4$)$_2$ transition, a more conservative approach was proposed by Paolone et al., who heated Ca(BH$_4$)$_2$·2THF at 125 °C for 20 h (incomplete conversion of THF adduct to α-Ca(BH$_4$)$_2$), followed by the α → α' structural phase transition at 180–220 °C, and finally the α'→β transformation at 320–330 °C [39]. Monitoring the vibration frequency of Ca(BH$_4$)$_2$ via anelastic spectroscopy measurements, the authors also noted that upon further cooling the sample from 320 °C to room temperature, the borohydride did not undergo any phase transitions, consistent with irreversible transformations occurring during heating (α → α' → β). Although not detected by DSC, evaluation of the relative variation/decrease of Young's modulus upon heating can indirectly point out these transitions [39]. Some debate still exists in the literature, as

some authors claim another phase in the C2/c space group for $Ca(BH_4)_2$ near ambient conditions [40].

Stoichiometric Equations (1)–(7) can describe several possible decomposition pathways for $Ca(BH_4)_2$ (Figure 1).
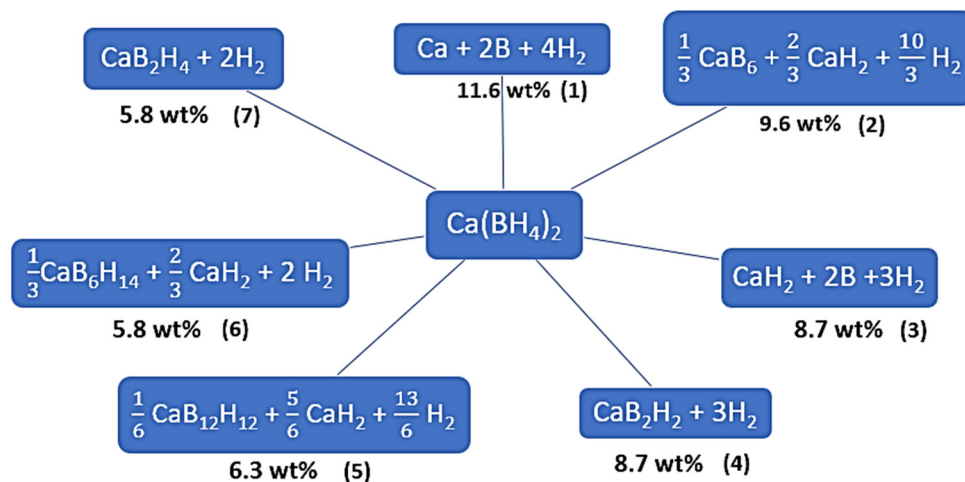
Figure 1. Decomposition pathways possible for calcium borohydride (Equations (1)–(7)).

Judging by how widespread dodecahydro-closo-dodecaborates ($B_{12}H_{12}^{2-}$) are during the dehydrogenation of metal borohydrides $M(BH_4)_n$, it seemed reasonable to further study the implications of these intermediate species on hydrogen storage properties as well as on the unexpected increase in ionic conductivity of related alkali and alkali-metal compounds [41]. Some representative examples of polymorphs of $Ca(BH_4)_2$, mixed anion borohydrides, and dodecaborate anion are depicted in Figure 2.
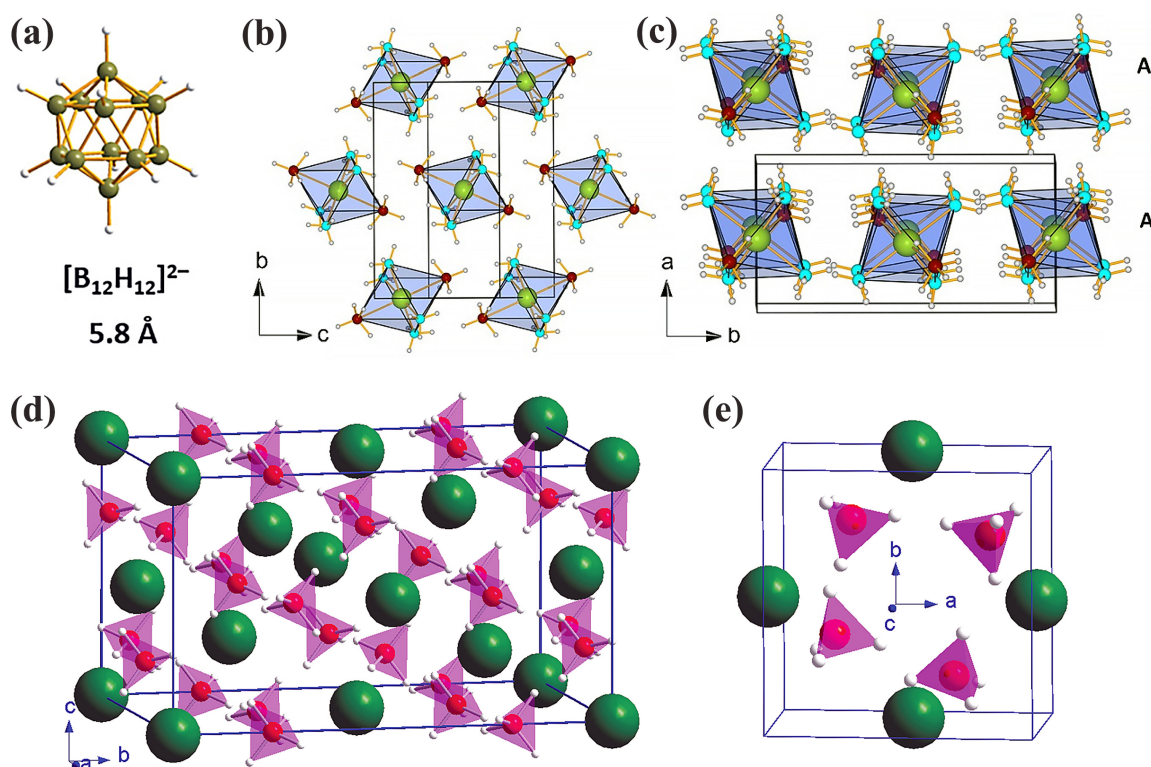
Figure 2. (**a**) Representation of the dodecahedral $[B_{12}H_{12}]^{2-}$ ion of the icosahedral frame. Boron atoms (green), hydrogen atoms (white). (**b**) Crystal structure of $Ca(NH_3)_4(BH_4)_2$. Ca, B, N, and H are represented by yellow, red, blue, and gray spheres, respectively; the molecular $[Ca(NH_3)_4(BH_4)_2]$

octahedra form hexagonal patterns in the bc plane. (**c**) The layers are stacked in the order AAA along the a direction (reproduced with permission from Ref. [15]). (**d**) Crystal structures of α-Ca(BH$_4$)$_2$ in space group *Fddd* and (**e**) β-Ca(BH$_4$)$_2$ in space group $P\bar{4}$. The color codes for atoms are green (calcium), pink (boron), and white (hydrogen). Each BH$_4^-$ unit is shown by a tetrahedron. Reprinted with permission from Ref. [38].

The thermal stability of MB$_{12}$H$_{12}$ is rather high, but a tendency towards amorphization (perhaps of the tentative formula B$_{12}$H$_{12-x}^{2-}$) has been recorded upon heating to 400–450 °C and further, when anion polymerization may occur (CaB$_y$H$_z$)$_n$, but elemental B was not observed even at 750 °C [41].

Jepsen et al. have recently described the DFT-optimized and experimental crystal structures (synchrotron radiation powder XRD data) of Ca(NH$_3$)$_n$(BH$_4$)$_2$ (n = 1, 2, 4, and 6) (Figure 3) [15]. DFT calculations were performed to optimize the structures from the SR-PXD data by using the Vienna Ab-initio Simulation Package (VASP) in the Perdew–Burke–Ernzerhof generalized-gradient approximation [15]. Ca(NH$_3$)$_4$(BH$_4$)$_2$ (*P21/c*) has a molecular structure connected by dihydrogen bonds, and all ammine complexes release ammonia upon gentle heating (at a low partial pressure of NH$_3$), or H$_2$-NH$_3$ (high partial pressure of NH$_3$). These findings suggest metal ammine borohydrides can be used to store ammonia, or to release H$_2$ by catalytic ammonia splitting [15].
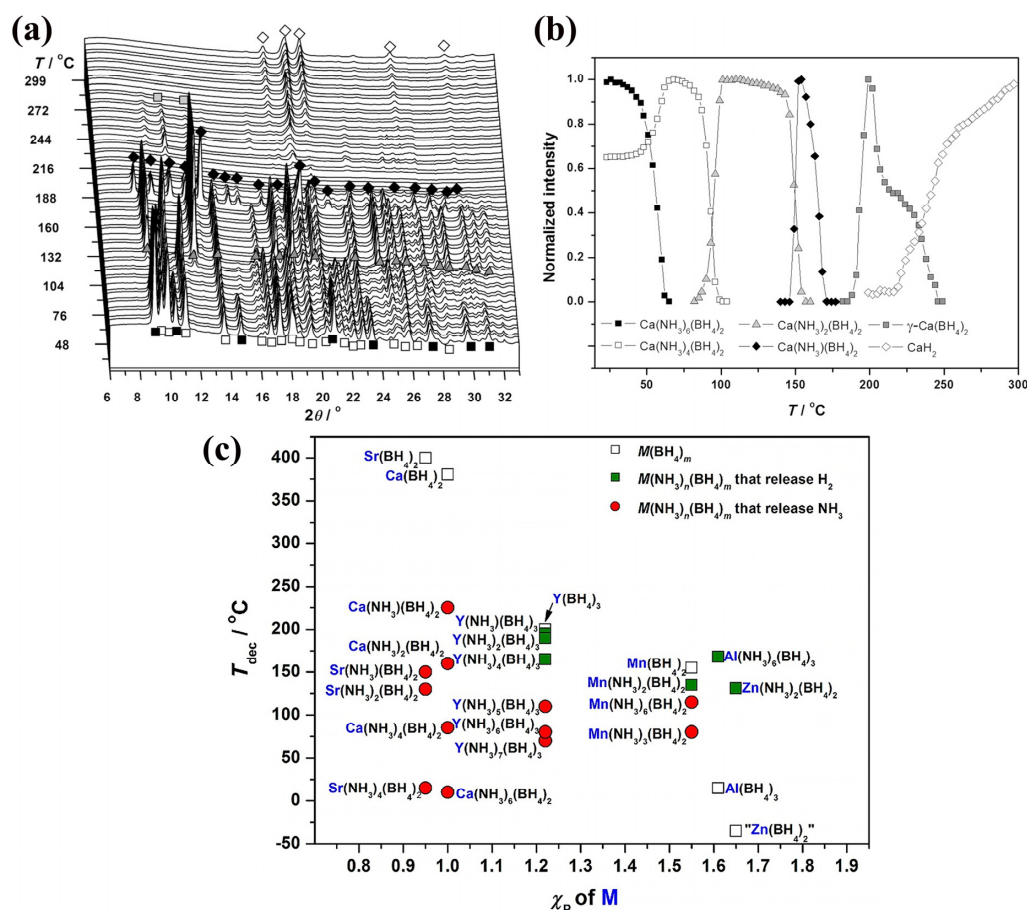
Figure 3. (**a**) In situ SR-PXD pattern of Ca(NH$_3$)$_6$(BH$_4$)$_2$ heated from RT to 350 °C (5 °C min^{-1}, p(Ar) = 1 bar, λ = 0.9941 Å). (**b**) Normalized integrated diffraction intensities plotted as a function of temperature. Reprinted with permission from Ref. [15]. (**c**) Decomposition temperatures for selected ammine metal borohydrides and the respective metal borohydrides under an Ar atmosphere, as a function of the metal M electronegativity. Zn(BH$_4$)$_2$ is not observed experimentally and is considered unstable. Reprinted with permission from Ref. [15].

Ca^{2+} is octahedrally coordinated to six equivalent [BH_4] tetrahedra, featuring Ca-B bond distances of 2.82–2.97 Å. The divalent cations in α-$Ca(BH_4)_2$ form a close-packed, diamond-type structure where the tetrahydroborate groups exhibit T-shape coordination.

Another interesting intermediate that can be observed during thermal decomposition of $Ca(^{11}BD_4)_2$; after initially being described as belonging to "δ-$Ca(BH_4)_2$", it has been properly assigned to $Ca_3(^{11}BD_4)_3(^{11}BO_3)$ and its structure was deduced by Riktor et al. based on synchrotron radiation powder XRD and supported by IR measurements [42].

With a decomposition enthalpy in the range 40.6–87 kJ/(mol H_2) and an onset decomposition temperature of 278 °C under 1 bar equilibrium pressure, bulk $Ca(BH_4)_2$ requires considerable modifications in order to conform to DOE's restrictions. Overcoming sluggish kinetics, problematic mass transfer, and high reaction enthalpies remain key steps needing further improvement.

3.2. Cation Substitution

Cation substitution has been pursued in dual-cation borohydrides in order to decrease the energy barriers in hydrogenation studies of calcium borohydride [43–47]. For instance, Fang et al. studied the dual-cation (Li, Ca) borohydride $LiCa(BH_4)_3$ [43]. The mixed borohydride was synthesized by ball milling a 1:1 mixture of $LiBH_4$:$Ca(BH_4)_2$, when an intermediate phase $Li_{0.9}Ca(BH_4)_{2.9}$ was observed to transform into the final stoichiometric mixed-cation borohydride $LiCa(BH_4)_3$ upon heating. The dual cation $Li_{0.9}Ca(BH_4)_{2.9}$ was produced most likely by incorporation of dissolved $LiBH_4$ into β-$Ca(BH_4)_2$ (Equation (10)).

$$LiBH_4 + Ca(BH_4)_2 \xrightarrow{\text{ball milling}} Li_{0.9}Ca(BH_4)_{2.9} + 0.1\ LiBH_4 \xrightarrow{\Delta} LiCa(BH_4)_3 \qquad (10)$$

Contrary to the desorption of individual borohydrides, the mixed-phase $LiCa(BH_4)_3$ started to desorb H_2 at 200 °C, considerably lower than the onset of $LiBH_4$ (400 °C) or $Ca(BH_4)_2$ (300 °C), and lost ~9.6 wt% after heating to 500 °C [43]. The Li-Ca-B-H system also bypassed the formation of the [$B_{12}H_{12}$]$^{2-}$ anion, following a two-step reaction that yielded 1.2 wt% and 8.1 wt% H_2, respectively (Equation (11)). The reversibility of the second dehydrogenation step was, however, only moderate, affording 5.3 wt% H_2 recharging [43].

$$LiCa(BH_4)_3 \xrightarrow{\Delta} LiCaB_3H_{11} + \frac{1}{2}H_2 \xrightarrow{\Delta} LiCa(BH)_3 + \frac{9}{2}H_2 \qquad (11)$$
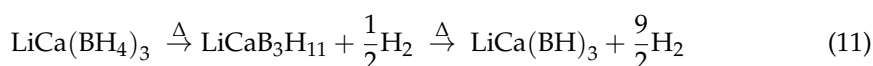
Jiang et al. observed a new mixed-borohydride adduct when mixing 3 $LiBH_4$:1 $CaCl_2$ in THF, namely, $LiBH_4 \cdot Ca(BH_4)_2 \cdot 2THF$, which released a mixture of H_2-B_2H_6 upon heating in a complex, 4-step process involving the detection of yet-unknown Li-Ca-B-H phases [44]. Although typically mixing metal halides such as MCl_n with $LiBH_4$ can yield mixed alkali metal-transition metal borohydrides (Equation (12)), a different reaction pathway was revealed when tuning the $CaCl_2$:$LiBH_4$ molar ration, while also using THF as reaction media.

$$MCl_n + m\ LiBH_4 \rightarrow MLi_{m-n}(BH_4)_m + n\ LiCl \qquad (12)$$

Additionally, $LiBH_4 \cdot Ca(BH_4)_2 \cdot 2THF$ was shown to store reversibly up to 5.63 wt.% H_2 in the second a/d cycle [44]. Switching $LiBH_4$ with $NaBH_4$, Mattox et al. have reported the influence of the borohydride starting material on the additive used (40% $CaCl_2$), concluding that $NaBH_4$ might interpenetrate the $CaCl_2$ lattice, expanding it [46]. The hypothesized product was marked as $CaNa(BH_4)_{1-x}Cl_x$, akin to the expected product based on Equation (12).

Lang et al. reported the decomposition of another substituted borohydride, the perovskite-type $NH_4Ca(BH_4)_3$ (15.7 wt.% hydrogen capacity, Equation (13)) [45]. The origin of the low desorption temperature (65 °C) was found to reside in the destabilization of H^+ in NH_4^+ and H^- in BH_4^- [45].

$$LiBH_4 + Ca(BH_4)_2 + NH_4Cl \rightarrow NH_4Ca(BH_4)_3 + LiCl \qquad (13)$$

The low onset correlates well with the reaction between NH_4^+ and BH_4^-, which takes place at 85 °C according to Equation (14).

$$NH_4^+ + BH_4^- \rightarrow NH_3BH_3 + H_2 \tag{14}$$
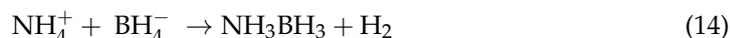
Upon heating, $NH_4Ca(BH_4)_3$ releases H_2 with the formation of $Ca(BH_4)_2NH_3BH_3$, an adduct that further desorbs ammonia borane AB: NH_3BH_3 (which undergoes a complex decomposition process also releasing H_2), and $Ca(BH_4)_2$ that can further react with LiCl to form anion-substituted borohydrides (Equation (15)) [45].

$$NH_4Ca(BH_4)_3 \xrightarrow{-H_2} Ca(BH_4)_3 \cdot NH_3BH_3 \xrightarrow{+LiCl,-AB} Ca(BH_4)_xCl_{2-x} + Li(BH_4)_yCl_{1-y} \tag{15}$$
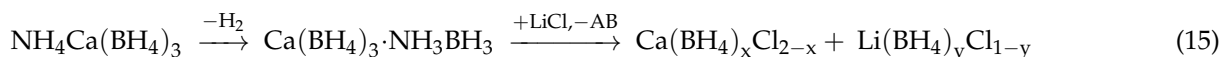
It appears that ~3.8 wt% H_2 can be released upon heating to 140 °C for 25 min, with very little other impurity gases such as NH_3 or B_2H_6 (Figure 4).
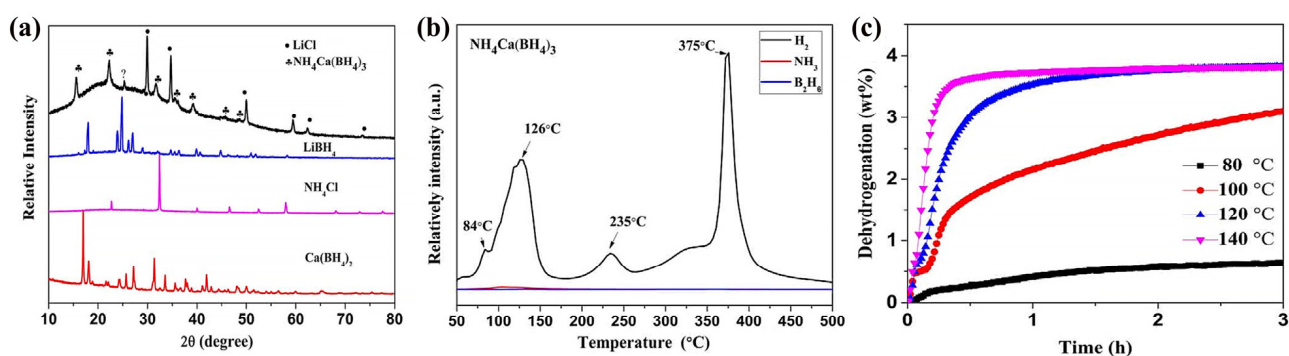
Figure 4. (**a**) XRD patterns of starting materials and as-milled samples; (**b**) MS profiles of $NH_4Ca(BH_4)_3$; (**c**) isothermal hydrogen desorption curves of $NH_4Ca(BH_4)_3$ at varied temperatures. Reprinted with permission from Ref. [45].

The previous study on $NH_4Ca(BH_4)_3$ in relation to the proposed destabilization borohydride-ammonium system, was reported by Schouwink et al. [47]. In addition to Equation (13), Schouwink used a novel approach: soft milling $Ca(BH_4)_2$ (30 min, 500 rpm) with temperature-stabilized NH_4BH_4 (cooling at 243 K) (Equation (16)).

$$NH_4BH_4 + Ca(BH_4)_2 \xrightarrow{ether} NH_4Ca(BH_4)_3 \tag{16}$$

The crystal structure of $NH_4Ca(BH_4)_3$ was also reported with a structural model in space group P-43m [47] (Figure 5).
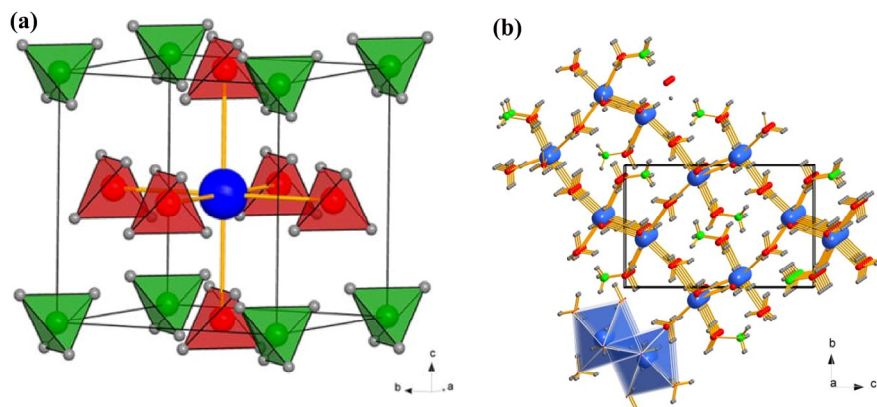
Figure 5. Structural models for (**a**) $NH_4Ca(BH_4)_3$ in space group P-43m; NH_4^+ (green), BH_4^- (red), Ca (blue0; and (**b**) $Ca(BH_4)_2 \cdot AB$; N (green), B (red), H (grey), Ca (blue). Reprinted with permission from reference [47].

3.3. Anion Substitution

Grove et al. have studied halide substitution in $Ca(BH_4)_2$ by ball milling the mixtures $Ca(BH_4)_2{:}x\ CaX_2$ (X = F, Cl, Br) with various molar ratios (x = 0.5, 1, 2) [48]. The compositions from x = 0–0.6 yield solid solutions of composition $\beta\text{-}Ca((BH_4)_{1-x}Cl_x)_2$ as revealed by Rietveld analysis of diffraction data, but there was no substitution of X^- for BH_4^- occurring for X = F or Br, possibly due to the positive enthalpy of mixing (X = F) or the lack of orthorhombic-to-tetragonal phase transition (X = Br) (Equation (17)) [48].

$$x\ CaCl_2 + \beta - Ca(BH_4)_2 \rightarrow (1+x)\ \beta - Ca((BH_4)_{1-x}Cl_x)_2 \tag{17}$$
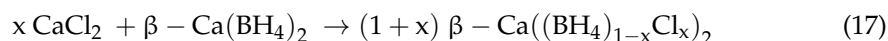
Even though DFT calculations predicted Br^- substitution to be possible, this possibility was experimentally discarded. Additionally, DSC of $\beta\text{-}Ca((BH_4)_{0.5}Cl_{0.5})_2$ showed a higher decomposition temperature compared to pure $Ca(BH_4)_2$. Interestingly, no substitution was observed at temperatures below 250 °C or in the case of $\alpha\text{-}Ca(BH_4)_2$, the only polymorph undergoing this substitution being $\beta\text{-}Ca(BH_4)_2$ (Figure 6) [48]. The calculations were performed applying the periodic quantum-mechanical software CRYSTAL09 within the density functional theory, PBE functional [48].
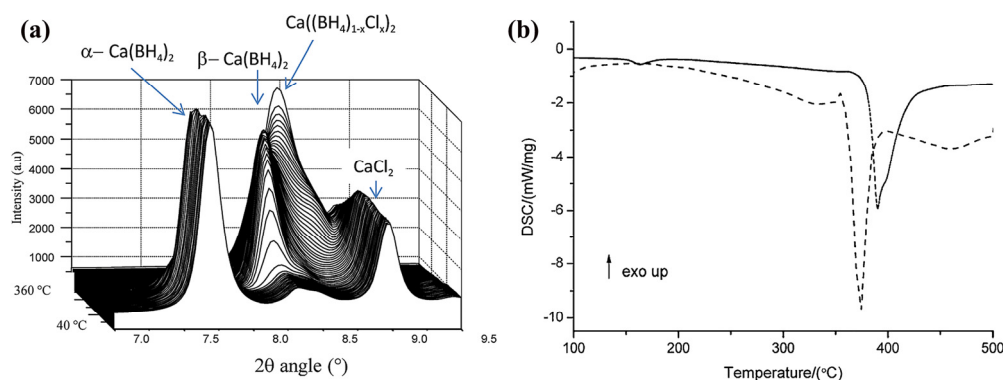
Figure 6. (**a**) In situ SR-PXD measured for $Ca(BH_4)_2+CaCl_2$ in molar ratio 1:1, heating rate 3 K min^{-1}. The temperature increases from 40 to 360 °C. (a) 3D plot of the selected 2θ area. Λ = 0.703511 Å; (**b**) DSC data for $Ca(BH_4)_2$ (dashed) and $Ca(BH_4)_2$–$CaCl_2$ (1:1) (solid) with a heating rate of 10 K min^{-1}. Reproduced with permission from Ref. [48].

Extending the range of calcium halides used for anion substitution in calcium borohydride, Rude et al. have employed CaI_2 in the system $Ca(BH_4)_2$–CaI_2 and found three new components formed by halide substitution: a solid solution $Ca((BH_4)_{1-x}I_x)_2$ with x~0.3, the trigonal $tri\text{-}Ca((BH_4)_{0.70}I_{0.30})_2$, and the orthorhombic $ort\text{-}Ca((BH_4)_{0.64}I_{0.36})_2$ [49]. The hydrogen release occurs from tetragonal $Ca((BH_4)_{1-x}I_x)_2$ via CaHI; however, the anion substitution strategy affords borohydrides with a decomposition temperature similar to that of $Ca(BH_4)_2$ [49].

3.4. DFT Computation and Predictions

Several DFT computation studies have surfaced related to calcium borohydride, from crystal structure under high pressure [50], predictive evaluation of mixed-anion $Ca(BH_4)(NH_2)$ [51], simulation of the nanosizing effect of $Ca(BH_4)_2$ [52], to the inclusion of metal borohydrides in a combined multidisciplinary approach aimed to further adjust hydride materials for vehicular applications [1]. Aidhy et al. have used a combination of density functional theory (DFT) calculations and a Monte Carlo (MC)-based crystal structure prediction tool, the Prototype Electrostatic Ground State (PEGS) method [51]. Albanese et al. have utilized for the theoretical investigation of $Ca\,(BH_4)_2$ the periodic density functional theory (DFT) calculations employing the PBE functionals as implemented in the CRYSTAL program, with the following all-electron basis set used for all the atoms, namely, 865-11G (2d) for Ca, 6-21G (d) for B, and 31G (p) for H [52]. Other studies have

investigated the metal electronegativity role in the $M(BH_4)_x$–$LiNH_2$ system as a means to enhance dehydrogenation thermodynamics and kinetics in the RHC [53]. Blanchard et al. have combined quasielastic neutron scattering (QENS) and DFT calculations to elucidate the role of hydrogen rotational and translational diffusion in calcium borohydride as an important factor of hydrogen dynamics in crystalline $Ca(BH_4)_2$ [54]. The calculations were performed by using the atomic simulation environment (ASE) package, and the DACAPO plane-wave basis-set implementation was used to solve the electronic structure problem within the DFT formalism; the ion cores were described by ultrasoft pseudopotentials, and the exchange and correlation effects were described by the PW91 functional [54].

Alkali-earth metal borohydride stability $M(BH_4)_2$ (M=Be, Mg, Ca) has been studied since the 1990s by Bonaccorsi et al. by systematic nonempirical calculations performed on $M(BH_4)_2$, $HMBH_4$, and $MBH_4{}^+$, resulting in optimized geometries [3]. Interestingly, the authors employed the effect of electron correlation in the study of the multi-step decomposition leading to borane elimination, an experimental detail observed in the case of many TM-based borohydrides (Equation (18)).

$$M(BH_4)_2 \rightarrow HMBH_4 + BH_3 \rightarrow MH_2 + 2\,BH_3 \rightarrow M + H_2 + 2\,BH_3 \tag{18}$$
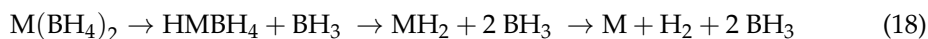
However, a critical point regarding DFT computations is that the agreement with experimental data must be reasonably good; with this goal in mind, Franco et al. used Quantum ESPRESSO to perform DFT computations on seven simple and complex hydrides (including $Ca(BH_4)_2$), and found that coupling the GIPAW (gauge-including projected augmented-wave) ab initio method with solid-state NMR experiments led to a good agreement among all investigated samples [55]. For example, [11]B MAS (Hahn echo) spectra of Ca(BH4)2 as a mixture of α and β phases showed corresponding signals at −32.5 pp (β phase) and −29.9 ppm (α phase), and ^{1}H SSNMR data also showed good correlation with prediction shifts (PAW: 0.48 ppm error, QE: 0.35 ppm error) (Figure 7) [55].
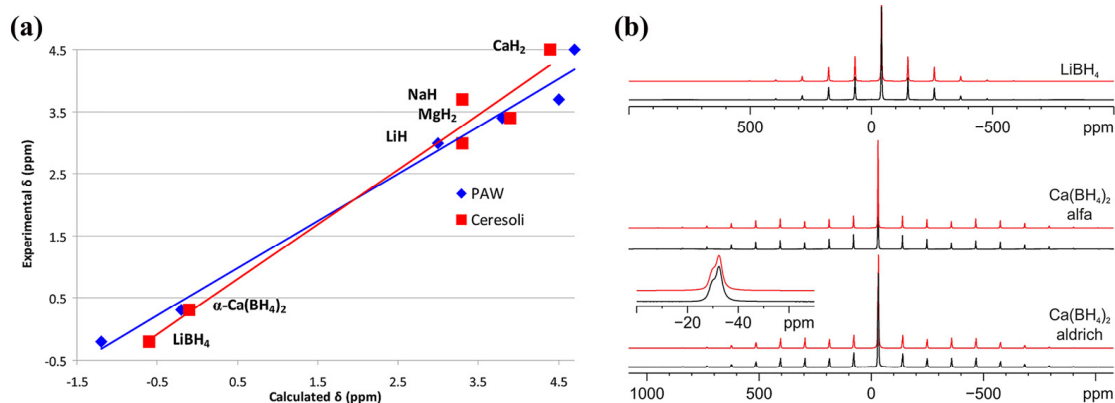
Figure 7. (**a**) Experimental vs. calculated ^{1}H chemical shifts (TMS as reference). (**b**) Experimental (black) and simulated (red) [11]B MAS (Hahn echo) spectra of α-$Ca(BH_4)_2$, and $Ca(BH_4)_2$ Aldrich (α + β form) recorded with a spinning speed of 14 kHz. Reproduced with permission from Ref. [55].

There is, however, an important need to develop new systems for energy storage, and Wolverton et al. employed an atomic scale computational approach using Perdew–Wang GGA (generalized gradient approximation) in this regard, with three-fold advances being recorded: the prediction of hydriding enthalpies and free energies, the prediction of favorable decomposition pathways, and the prediction of low-energy crystal structures of complex hydrides [12]. The results suggest that the DFT approach is useful in evaluating potential decomposition pathways, as was exemplified for $Li_4BN_3H_{10}$, a metastable phase with three potential decomposition pathways for T < 300 K and thermodynamically possible with $\Delta G < 0$ [12].

4. Characterization and Stability

As previously mentioned, there are several early reports related to the structure and stability of calcium borohydrides [3,35,56]. For instance, Filinchuk et al. [35] and Bosenberg et al. [57] reported the characterization of metal hydride using in situ synchrotron radiation powder X-ray diffraction (SR-PXD). SR-PXD is a powerful tool to track solid-gas reactions, and hydrogenation studies made use of a cell that allows control over wide pressure and temperature ranges (up to 200 bar, 550 °C) [57–59]. The authors reported that β-Ca(BH$_4$)$_2$ and MgH$_2$ were observed when a mixture of CaH$_2$-MgB$_2$ was heated, as well as the β → α phase transition of calcium borohydride upon cooling [57]. Dematteis et al. deduced the heat capacities and thermodynamic properties of complex hydrides, which will further ease the thermodynamic data computations (ΔS, ΔH and ΔG) [60].

Other physical characterization methods include inelastic neutron scattering [61], high-resolution laser excitation spectroscopy (albeit for hypothetical, gas phase CaBH$_4$ molecule) [62], vibrational spectra (IR and Raman, for α-, β-, and mixed (β,γ)-Ca(BH$_4$)$_2$) [38,63,64], solid-state NMR (^{1}H, ^{11}B MAS for α-, β-Ca(BH$_4$)$_2$ [29,55,65], confirmation of [B$_{12}$H$_{12}$]$^{2-}$ species during borohydride dehydrogenation [66], ^{11}B spin-lattice relaxation [67], analysis of RHCs based on calcium borohydride like LiBH$_4$–Ca(BH$_4$)$_2$ [68]), and various DFT computations (excluding CaB$_2$H$_2$ as dehydrogenation intermediate, while favoring CaB$_{12}$H$_{12}$ as an intermediate, as argued by Frankcombe, Equation (19) [69], or evaluating [Ca(BH$_4$)$_2$]$_{n=1-4}$ clusters for hydrogen storage by Han et al. [70]).

$$Ca(BH_4)_2 \rightarrow \frac{1}{6}CaB_{12}H_{12} + \frac{5}{6}CaH_2 + \frac{13}{6}H_2 \rightarrow \frac{1}{3}CaB_6 + \frac{2}{3}CaH_2 + \frac{10}{3}H_2 \qquad (19)$$
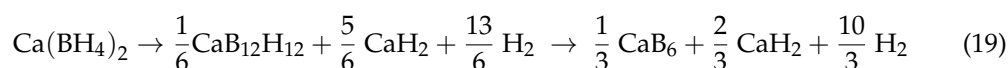
Hattrick-Simpers et al. described the use of high-throughput backscattering Raman spectroscopic measurements for combinatorial in situ Raman spectroscopy of Ca(BH$_4$)$_2$ and other RHCs (up to 10 Mpa and 823 K) [71].

The stability of Ca(BH$_4$)$_2$ has been investigated in many reports, including Miwa et al. [72], Nakamori et al. [73], Riktor et al. [58], and others. Since the decomposition of complex hydrides is related to their hydrogen storage capacity, these results will be discussed in Section 5.

4.1. Neat vs. Nanoconfined

Several aspects of nanosizing are regarded as beneficial for enhancing de-/rehydrogenation of complex hydrides and related RHCs. For instance, when impregnating LiBH$_4$ into ferrite-catalyzed-graphene, a synergistic effect was observed and an important reduction in activation energy was recorded [74].

4.2. DFT Simulation of the Nanosizing Effect

Albanese et al. have studied the nanostructuring of β-Ca(BH$_4$)$_2$ by atomistic thin film models to mimic nanosizing effects (DFT, using CRYSTAL software) in order to evaluate the reduction of dehydrogenation enthalpy of calcium borohydride, showing that for thickness in the range 5–20 Å, the reduction on enthalpy reaches 30–35 kJ/mol H$_2$, making calcium borohydride an appealing candidate for hydrogen storage under nanosizing conditions [52]. The decomposition pathways for Ca(BH$_4$)$_2$ have been investigated by Zhang et al. by means of DFT calculations of free energy, predicting a new CaB$_2$H$_6$ compound as a decomposition intermediate [75]. Other groups have evaluated the effectiveness of DFT computations in establishing metastable reaction pathways [76].

Dual-cation borohydrides of form M$_1$M$_2$(BH$_4$)$_3$(NH$_3$)$_{2-6}$ have been investigated by Emdadi et al., finding several potentially promising new solvates and stable alloys, including M$_2$=Ca [77]. Nanosizing was invoked in the case of LiBH$_4$–Ca(BH$_4$)$_2$ RHC when catalyzed by LaMg$_3$, with an improvement registered in hydrogenation behavior due to nanoparticulate alloy addition affording a dehydrogenation onset at ~200 °C, 100° lower than pristine LiBH$_4$–Ca(BH$_4$)$_2$ and rehydrogenation proceeding at 150 °C [78].

Guo et al. performed first-principles calculations on the system $KBH_4/Ca(BH_4)_2$ and proposed three new reactions in the mentioned RHC (20), (21) and (22), two of them involving the formation of the $[B_{12}H_{12}]^{2-}$ anion [79,80].

$$KBH_4 + \frac{5}{2} Ca(BH_4)_2 \rightarrow \frac{1}{2} K_2B_{12}H_{12} + 5\, NaH + \frac{13}{2} H_2;\ 6.0\ wt\%\ t_c = 64\ ^\circ C \qquad (20)$$

$$KBH_4 + \frac{1}{10} Ca(BH_4)_2 \rightarrow \frac{1}{10} CaB_{12}H_{12} + KH + \frac{13}{10} H_2;\ 4.3\ wt\%\ t_c = 58\ ^\circ C \qquad (21)$$

$$KBH_4 + \frac{1}{4} Ca(BH_4)_2 \rightarrow \frac{1}{4} CaB_6 + KH + \frac{5}{2} H_2;\ 7.0\ wt\%\ t_c = 105\ ^\circ C \qquad (22)$$
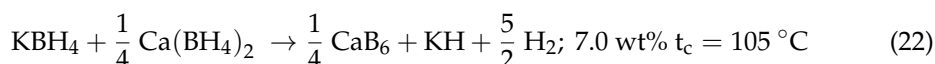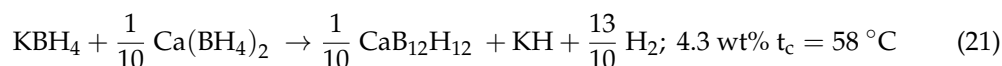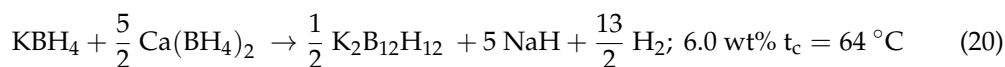
Moreover, Kulkarni et al. described by first principles the dodecaborane, amorphous phase $CaB_{12}H_{12}$ as a result of an overlap of structurally distinct crystallites [81].

Huang et al. performed first-principles calculations involving Cr-doping of α-$Ca(BH_4)_2$ and found half-metallic behavior (0.98 eV for Ca doped sites, 0.63 eV for B) useful for further use in spintronic devices [82]. Computational thermodynamics coupled with CALPHAD (CALculation of PHAse Diagram) modeling revealed the formation of $Ca(BH_4)_2$ as a result of Ca addition on $LiBH_4$, along with CaB_6, which significantly reduces the H_2 releasing temperature of the system [83].

The utilization of $Ca(BH_4)_2$ in electrolyte solution for Ca-ion batteries has been shown feasible by a computational approach called AIMD (ab initio molecular dynamics) performed on ether- and ester-based electrolytes on a calcium anode, revealing an aspect that was confirmed experimentally, namely, that the best combination for an electrolyte solution is that of $Ca(BH_4)_2$ and the polar, aprotic THF solvent [84]. Calcium borohydride ($Ca(BH_4)_2$) has shown potential for use in both lithium-ion batteries (LIBs) and sodium-ion batteries (SIBs) due to its high hydrogen storage capacity and favorable electrochemical properties. Regarding LIBs, it must be noted that $Ca(BH_4)_2$ can release H_2 through a reversible electrochemical process, enabling its use as an energy and H_2 reservoir within the battery. The high capacity of $Ca(BH_4)_2$ for Li storage (by theoretical calculations, one mole of $Ca(BH_4)_2$ can potentially store four moles of lithium, leading to a high energy density) makes it an attractive solution for LIB applications. However, compared to $Mg(BH_4)_2$, which afforded 540 mAh/g (first discharge)/250 mAh/g (recharge), the reported values for $Ca(BH_4)_2$ were lower. With good chemical stability, calcium borohydride showed good stability during lithium insertion/extraction, therefore showing good potential for long term cycling stability. Several downsides should be addressed, such as developing the proper electrolyte system that would afford better overall battery performance and stability. As with LIBs, SIBs show similar advantages and downsides for $Ca(BH_4)_2$ use in battery applications.

Mikhailin et al. employed potential energy surfaces along minimal energy pathways to study the decomposition of $M(BH_4)_2(NH_3)_{1-2}$ and the $[M(BH_4)_2(NH_3)_2]_2$ dimers (M=Be, Mg, Ca, and Zn) using the B3LYP method (DFT). The dimeric structures have almost no effect on the energy barriers, while coordination of the ammonia molecule to the metal center reduced these barriers considerably, affording dehydrogenation at temperatures much lower than those of their corresponding pristine counterparts [85]. The potential decomposition pathways of calcium ammine borohydride complexes would lead to $Ca(BH_2NH)(BHN)$, $Ca(BH_4)(BHN)$ or $Ca_2(BH_4)_2(NH_3)_2(BH_3NH_2)_2$ in the case of the dimer [85]. The case of decomposition of $Ca(BH_4)_2 \cdot NH_3$ was further investigated by Zhang et al. by means of DFT and showed a reasonable agreement with decomposition in the range 190–250 °C, releasing 11.3 wt% hydrogen [86]. Notably, the interaction N-H . . . H-B was found to play an essential role in favoring H_2 release, recognizing the unique role of dihydrogen bonding in H_2 release from solid compounds such as complex hydrides and their adducts [86]. Various complementary predictions have been made on the basis of thermodynamic computations by Siegel et al. [87], and Vajeeston et al. [88,89].

4.3. Destabilization Strategies

Destabilization of boron-based materials can be achieved by using additives (various compounds based on Mg, B, Al, C, S, Ti, intermetallics, etc.), chemical modifications, and nanosizing effects [90–98]. Various RHCs have been employed, and most showed improved desorption temperatures compared to pristine components; for instance, $Mg(BH_4)_2/Ca(BH_4)_2$, $Mg(BH_4)_2/CaH_2$, or $Mg(BH_4)_2/CaH_2/3NaH$ (Equations (23)–(25)) (Figure 8) [92,94].

$$5\,Mg(BH_4)_2 + Ca(BH_4)_2 \rightarrow CaB_{12}H_{12} + 5\,MgH_2 + 13\,H_2 \tag{23}$$

$$3\,Mg(BH_4)_2 + CaH_2 \rightarrow 3\,MgH_2 + CaB_5 + 10\,H_2 \tag{24}$$

$$3\,Mg(BH_4)_2 + CaH_2 + 3\,NaH \rightarrow 3\,NaMgH_3 + CaB_5 + 10\,H_2 \tag{25}$$
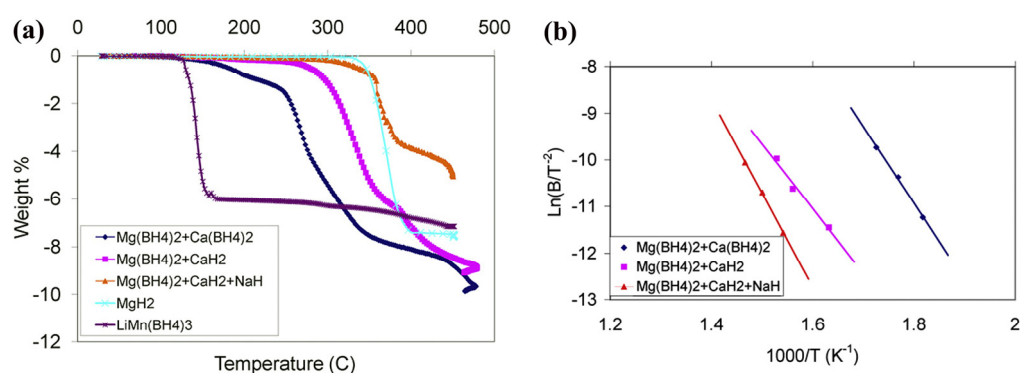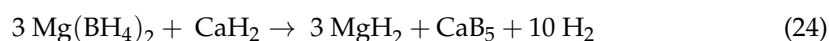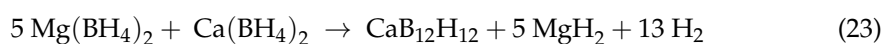
Figure 8. (**a**) TPD profiles comparing the desorption temperatures of several solid-state hydrogen storage materials. (**b**) Activation energy plots using the Kissinger equation for several mixtures. Reprinted with permission from Ref. [92].

Ibikunle et al. also studied the RHC $Mg(BH_4)_2/Ca(BH_4)_2$ and found the H_2 release to be diffusion- and phase boundary-controlled (Figure 9) [94,95].
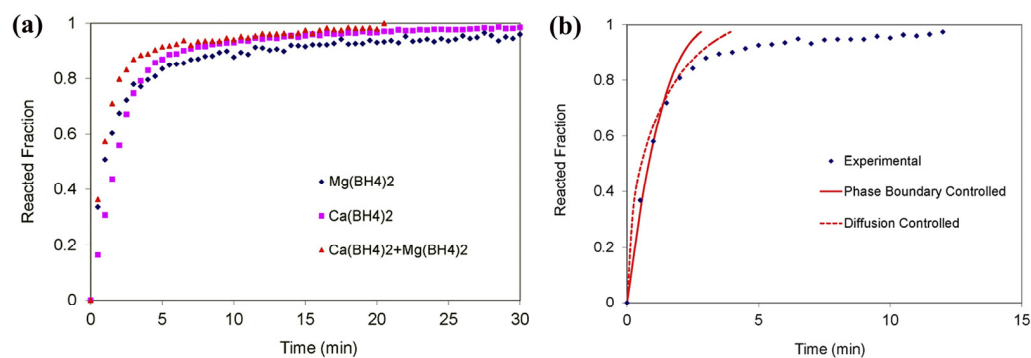
Figure 9. (**a**) Plots of reacted fraction versus time for $Mg(BH_4)_2$, $Ca(BH_4)_2$, and the $Mg(BH_4)_2/Ca(BH_4)_2$ mixture at 450 °C. (**b**) Modeling curves for $Mg(BH_4)_2/Ca(BH_4)_2$. Reprinted with permission from reference [94].

An extension of the destabilization strategy proposed by Durojaiye in 2010 [92] was employed by Huang et al. in 2016, who used $Mg(AlH_4)_2$ in order to destabilize $Ca(BH_4)_2$ instead of magnesium borohydride [93]. The destabilization effect of magnesium alanate $Mg(AlH_4)_2$ in the 1 $Mg(AlH_4)_2$:1 $Ca(BH_4)_2$ RHC was quantified and shown to exhibit a 10-fold faster desorption at 300 °C (0.337 wt.% H_2/min) compared to pristine $Ca(BH_4)_2$ (2.6 wt% H_2 at the same temperature), releasing 8.4 wt% H_2 at 330 °C in a three-step reaction (with release peaks at 130, 280, and 310 °C) [93]. A key step in the enhancement observed

was attributed to the formation of the Al (Mg) solid solution, effectively destabilizing $Ca(BH_4)_2$ [93].

Destabilization in the system $NaBH_4/Ca(BH_4)_2$ has also been reported (Equation (26)), and the TPD release curves were altered by a decomposition product of $Ca(BH_4)_2$; the system behaved reversibly under ~5.5 Mpa H_2 at 400 °C when recharged for 10 h [97].

$$4\,NaBH_4 + Ca(BH_4)_2 \rightarrow 4\,Na + CaB_6 + 12\,H_2;\ 10.9\ wt\%\ H_2 \qquad (26)$$

An important aspect of the reversibility reaction of many metal borohydrides is the regeneration of B–H bonds present in the $[BH_4]^-$ anion [90]. This issue was tackled by Cai et al., who proposed a general route potentially applicable to $M(BH_4)_2$ as well (M=Mg, Ca), based on the reaction of SiB_4 with $MH_{n=1-2}$ to form $M(BH_4)_{n=1-2}$ under mild conditions in the case of $LiBH_4$ (10 Mpa, 250 °C) (Equation (27)). The chemical bonding of boron in the reagent (SiB_4) was found essential for the best hydrogenation performance; for comparison, the synthesis of $LiBH_4$ from the elements requires 700 °C, while the mildest conditions are required by the solid-gas reaction between LiH and B_2H_6, yielding $LiBH_4$ at 120 °C.

$$SiB_4 + 4\,LiH + 6H_2 \rightarrow 4\,LiBH_4 + Si\ ;\ \Delta H = -65\frac{kJ}{molH_2} \qquad (27)$$
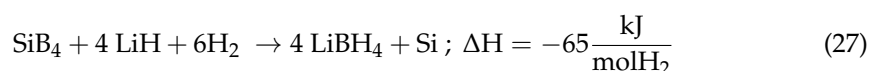
5. Hydrogen Storage Properties

Various aspects related to hydrogen desorption behavior have been investigated in recent years, from the detailed decomposition of pristine calcium borohydride by Kim et al. [99,100], to the kinetic and thermodynamic investigation of $Ca(BH_4)_2$ decomposition [101], to the further decomposition behavior of the $CaB_{12}H_{12}$ intermediate [66] or the debated formation of the CaB_2H_x intermediate reported by Riktor et al. [102]. Other reports shed light on the H_2 backpressure effect [100] or the dehydrogenation temperature used (350 °C vs. 400 °C), which can allow different pathways for the decomposition reaction (via CaB_2H_6 at 350 °C, or via B and CaH_2, leading to CaB_6 when heated at 400 °C) [103,104]. Further experimental details related to the H_2 desorption potential of $Ca(BH_4)_2$ will be discussed in the following sections (Sections 5.1–5.6), as well as the applicability of calcium borohydride to ion conductivity studies and applications (Section 5.7).

5.1. Bulk Ca(BH$_4$)$_2$

As early as 2008, Aoki et al. investigated the hydrogen release properties of $Ca(BH_4)_2$ and reported the phase transition (LT, low temperature, to HT, high temperature), while also identifying an unassigned intermediate compound and CaH_2 as the final phase identified by XRD data analysis [105]. Decomposition of pristine calcium borohydride has been thought and further demonstrated to proceed through the formation of $CaB_{12}H_{12}$ [14,66] or another intermediate type of the general formula CaB_2H_x (DFT computations) [34]. A pressure investigation performed on a mixture α- and β-$Ca(BH_4)_2$ led George et al. to identify a novel phase in which the β– phase transforms when reaching 10.2 Gpa, but no α-to-β transition was observed around 5.3 Gpa, as theoretically predicted [106]. Other DFT computations were run on $[Ca(BH_4)_2]_{n=1-4}$ clusters and found the smallest dissociation energy to belong to the tetramer $[Ca(BH_4)_2]_4$, indicative of it being the better hydrogen storage candidate among the investigated clusters [70].

The dehydrogenation of $Ca(BH_4)_2$ and that of the destabilized system $Ca(BH_4)_2$–MgH_2 were investigated by Kim et al., highlighting the essential role of the CaB_6 product in achieving system reversibility [107], as corroborated by the findings of Sahle et al. a few years later [108]. It was also suggested that CaB_6 forms as the final product of the reaction from intermediate phases likely containing B and CaH_2 [108].

As for the decomposition of $CaB_{12}H_{12}$, the decomposition pathway differs from that of $Ca(BH_4)_2$, producing no CaB_6, and can be described by Equation (28) [14]:

$$CaB_{12}H_{12} \xrightarrow{-\frac{x}{2}H_2} CaB_{12}H_{12-x} \xrightarrow{-\frac{z}{n}H_2} \frac{1}{n}\left(CaB_yH_z\right)_n \tag{28}$$
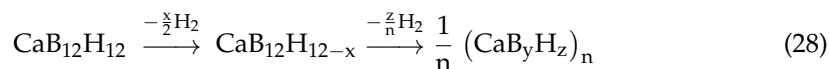
Moreover, although there are conflicting reports regarding the role of $CaB_{12}H_{12}$ in the dehydrogenation of $Ca(BH_4)_2$, it seems unlikely that the dodecaborate is a stable dehydrogenation intermediate [14,37].

5.2. Nanoconfined

Nanoconfinement remains a viable route for tuning the thermodynamic parameters of hydrogen storage materials and of $Ca(BH_4)_2$ in particular, with several reports describing marked improvements over the pristine compounds' thermal behavior [68,74,96,109–118]. Some of the most important characteristics of these systems are summarized in Table 2. A porous borohydride, CaB_2H_7, was obtained by heating $Ca(BH_4)_2$ with $Ti(Oet)_4$ at 160 °C for 1 h and showed improved release and uptake of hydrogen (Equation (29)) [112].

$$Ca(BH_4)_2 + 0.1\,Ti(OEt)_4 \xrightarrow{160\,°C,\,1\,h} CaB_2H_7\,0.1TiO_2 + 0.2\,C_2H_6 + 0.2\,C_2H_6O + 0.2\,H_2 \tag{29}$$

The desorption of the porous borohydride occurred in the 300–420 °C interval, following a two-step dehydrogenation pathway (Equation (30)) [112].

$$CaB_2H_7 \xrightarrow{300\,°C,\,1\,h} 0.6\,CaB_2H_4 + \frac{2}{15}CaB_6 + \frac{4}{15}CaH_2 + 3.8\,H \xrightarrow{420\,°C,\,1\,h} \frac{1}{3}CaB_6 + \frac{2}{3}CaH_2 + 5.7\,H \tag{30}$$
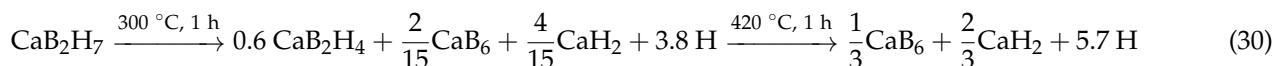
When $LiBH_4$ is used in the eutectic mixture $0.7\,Li(BH_4)_2$-$0.3\,Ca(BH_4)_2$ displaying eutectic melting, the reversible coupled RHC system obeys the reversible pathway described by Equation (31).

$$4\,LiBH_4 + Ca(BH_4)_2 \rightarrow CaB_6 + 4\,LiH + 10\,H_2 \tag{31}$$
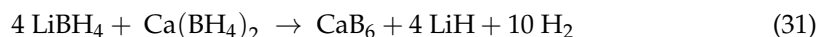
Other studies have focused on the infiltration and interaction between the eutectic $LiBH_4$–$Ca(BH_4)_2$ and mesoporous scaffolds (CMK–3, MCM–41) by means of NMR investigation, including the lack of surface modification of the inert carbon scaffold CMK-3, as revealed by ^{13}C MAS and ^1H-^{13}C CPMAS (cross-polarization MAS) spectra [68]. Other studies have used mesoporous silica as the host (MCM–41 and SBA–15) for $LiBH_4$–$Ca(BH_4)_2$ infiltration and found that the mesoporous structure of the scaffold was altered even with low-energy ball milling [115] or reported on the infiltration of the same RHC into mesoporous carbon [116]. One should also note the affinity of the borohydride for the SiO_2 and surface silanol groups, which may lead to another side reaction [115].

Table 2. Hydrogen storage characteristics of nanocomfined $Ca(BH_4)_2$ and its RHCs.

Ca-Based Storage Material	Nanoscaffold Used	wt% H₂ Storage Performance	Obs. (Reversibility, Catalyst)	Ref.
$Ca(BH_4)_2$ in CMK-3/$Ca(BH_4)_2$/$TiCl_3$	CMK-3 with S_{BET} = 1320 m²/g, V_p = 1.48 cm³/g (wet impregnation from NH_3 liq. solution to 70% pore filling)	H_2 release onset at 150 °C	$TiCl_3$ as catalyst (1:0.05 molar)	[110]
$Ca(BH_4)_2$ in Ca.$(BH_4)_2$=MC-a	MC-a (activated mesoporous carbon 1780 m²/g, 1.01 cm³/g); incipient wetness method	2.4 (reversible after 18 cycles)	Desorption onset at ~100 °C	[111]
$Ca(BH_4)_2$ in Ca.$(BH_4)_2$=MCM–41	MCM–41 (2.4 nm) and fumed silica (7 nm); wet infiltration	–	^1H and ^{11}B VT MAS NMR technique	[113]

Table 2. *Cont.*

Ca-Based Storage Material	Nanoscaffold Used	wt% H$_2$ Storage Performance	Obs. (Reversibility, Catalyst)	Ref.
Ca(BH$_4$)$_2$ in Ca.(BH$_4$)$_2$=rGO	Graphite and rGO (reduced graphene oxide); ball milling	6.5%	a 50 °C reduction in decomposition onset (220°, graphite; 170 °C, rGO)	[117]
0.7 Li(BH$_4$)$_2$-0.3 Ca(BH$_4$)$_2$ (eutectic mixture); ball milling (120 min, BPR 1:18)	CMK–3 mesoporous carbon (5 nm), ASM carbon (20–30 nm), and CD (non-porous carbon disks 20–50 nm thick, 0.8–3 µm diameter)	3.96 (CMK-3), 4.88 (ASM), 6.07 (CD)	Kinetic improvements when pore size ~5 nm, synergically coupled with a catalytic effect	[109]
0.7 Li(BH$_4$)$_2$-0.3 Ca(BH$_4$)$_2$ (eutectic mixture)	Two resorcinol-formaldehyde carbon aerogel scaffolds (pristine CA 689 m^2/g, CO$_2$-activated CA–6, 2660 m^2/g); 60 vol.% pore filling; melt infiltration method	Up to 12.08 % pristine (7.71% CA–6, 3.36% CA)	Reduced E$_A$ from 204$_{bulk}$ to 156$_{CA}$ and 130$_{CA-6}$ kJ/mol	[114]
CaB$_2$H$_7$/0.1TiO$_{2,nano}$ via Ca(BH$_4$)$_2$ + Ti(Oet)$_4$	Porous Ca-based hydride with in situ TiO$_2$ catalyst	6.2 % (300–420 °C, 1 h)	Recharge at 350 °C, 90 bar H$_2$, 1 h	[112]
0.68LiBH$_4$–0.32Ca$_{(BH4)}$2 in LiBH$_4$–Ca(BH$_4$)$_2$–NbF$_5$@CMK-3 composite	Catalyzed mesoporous carbon host, NbF$_5$@CMK-3	13.3% (250 min) vs. 10.4% (pristine RHC)	Desorption onset reduced by 120 °C compared to pristine	[37]

5.3. Additives Used to Improve H$_2$ Storage Features of Calcium Borohydride

While still holding the highest theoretical hydrogen storage capacity of all known materials, complex hydrides still face many shortcomings related to sluggish kinetic and/or thermodynamic barriers that are hard to bypass. To tackle this issue, several additives have been used, with important improvements recorded: MgB$_2$ yielded Ca(BH$_4$)$_2$ + MgB$_2$ composite with 8.3 wt% gravimetric hydrogen capacity [119]; Co ion-loaded poly(acrylamide-co-acrylic acid) (p(Aam-co-Aac)-Co) hydrogel when a decrease in conversion rate from 98.5 to 83.5% was reported over ten a/d cycles [120,121]; urea yielded a new complex hydride Ca(BH$_4$)$_2$·4CO(NH$_2$)$_2$, releasing 5.2 wt% hydrogen below 250 °C [122]; 5 wt% CoCl$_2$ doping in Ca(BH$_4$)$_2$-4LiNH$_2$ afforded catalyzed RHC (Co NPs formed during ball milling as active catalytic species), releasing 7 wt% hydrogen at 178 °C [123]; CoCl$_2$-doped Ca(BH$_4$)$_2$·2NH$_3$ desorbed at 200 °C, releasing 7.6 wt% H$_2$ with high purity [124]; Mg(BH$_4$)$_2$ yielded corresponding RHCs Mg(BH$_4$)$_2$/Ca(BH$_4$)$_2$ [92], MgF$_2$ in Ca(BH$_4$)$_2$-MgF$_2$ reversible system [125]; in situ generated TiO$_2$ to afford novel CaB$_2$H$_7$/0.1TiO$_2$ catalyzed hydride system [112]; particulate LaMg$_3$ additive in the RHC Ca(BH$_4$)$_2$ + LiBH$_4$ [78]; DFT investigation on Cr-doped α-Ca(BH$_4$)$_2$ [82]; TiF$_3$ introduced via ball milling in Ca(BH$_4$)$_2$ [126]; NbF$_5$ doping in Ca(BH$_4$)$_2$ + MgH$_2$ [127]; Nb and Ti doping on Ca(BH$_4$)$_2$ investigated by DFT [128]; Co-Ni-Fe-P alloy as hydrolysis catalyst [129]; TiCl$_3$ doping of Ca(BH$_4$)$_2$ yielded 2 wt% H$_2$ reversible at 300 °C and 9 Mpa, while also suppressing borohydride melting [103]; 10 mol% addition of CaX$_2$ (X=F, Cl) produced Ca(BH$_4$)$_2$–CaX$_2$ mixtures, where CaX$_2$ changed the dehydrogenation pathway [130].

Other reports deal with the additive role of calcium borohydride in the Mg(NH$_2$)$_2$–2LiH–0.1Ca(BH$_4$)$_2$ system, yielding CaH$_2$ and LiBH$_4$ during ball milling to account for 4.5 wt% storage capacity [131]; TiF$_4$ and NbF$_5$ doped in Ca(BH$_4$)$_2$-MgH$_2$ RHC, where a slight improvement was seen in the case of NbF$_5$ doping, and there was evidence of CaB$_{12}$H$_{12}$ formation along with the formation of active metal boride nanoparticulate species TiB$_2$ and NbB$_2$ (XANES data) with partial reversibility reported [132–134]; Ti(O^{i}Pr)$_4$ and CaF$_2$ [134]; TiF$_3$ additive in the 2NaAlH$_4$ + Ca(BH$_4$)$_2$ system generating Al$_3$Ti and CaF$_2$ with a synergistic catalytic role and affording improved a/d kinetics [135]; investigation of the boron effect in the Ca(BH$_4$)$_2$ + B system, showing only minor differences in the

maximum rate of H_2 evolution [136]; CaF_2 replacement of CaH_2 in $CaH_2 + MgB_2$ yielding the nonstoichiometric $CaF_{2-x}H_x$ solid solution with a direct influence over a/d behavior of the system [137]; TiX_3 (X=F, Cl) showing a superior effect of TiF_3 on reversibility (57% yield) but not of $TiCl_3$, despite their electronic similarities [138].

The catalytic role of additives in the synthesis of calcium borohydride from caB_6 and CaH_2 was confirmed by Ronnenbro et al. utilizing $RuCl_3$ or, even better, mixtures of $TiCl_3$ + Pd [11]. Another synthesis route of calcium borohydride starts from the $CaH_2 + MgB_2$ system, where the beneficial role of the boride additive AlB_2 was reported by Schiavo et al. [139], or the role of fluoride-based additives in the same $CaH_2 + MgB_2$ system, as shown by Suarez-Alcantara et al., who investigated the systems $9CaH_2 + CaF_2 + 10MgB_2$, $10Ca(BH_4)_2 + 9MgH_2 + MgF_2$, and $9Ca(BH_4)_2 + Ca(BF_4)_2 + 10MgH_2$ [59].

5.4. RHCs—Reactive Hydride Composites Containing Ca(BH$_4$)$_2$ or Its Precursors

There have been many attempts to catalyze $Ca(BH_4)_2$ and its RHCs; however, not all of them showed palpable results. For instance, while MgH_2 was considerably improved using Ni (5 wt%) and Ni_5Zr_2 (5 wt%) catalysts, these catalysts showed very little influence over $Ca(BH_4)_2$ [140]. On the other hand, the system $Ca(BH_4)_2$–MgH_2 was shown to produce the species $Ca[B_{12}H_{12}]$ [141]. The same $Ca(BH_4)_2$–MgH_2 RHC (10.5 wt% H_2 theoretical, 6.4 wt% H_2 desorbed within 3 h) has been characterized when catalyzed by 0.05 mol TiF_4 and NbF_5, yet the catalyst employed did not suppress dodecaborane anion formation, and only some minor improvements were recorded in the case of the NbF_5 catalyst's usage of TM fluorides, as shown by XANES data to form TM boride nanoparticles acting as active catalysts [132]. Minella et al. have also extended the study of $Ca(BH_4)_2$–MgH_2 RHC by using Mg, which behaves as an adjuvant for heterogeneous nucleation of CaB_6 formed during desorption [142]. CaB_6 formation was also reported in the RHC $6LiBH_4 + CaH_2$ (11.7 wt% theoretical), which afforded 9.1 wt% reversible storage capacity when catalyzed by 0.25 mol $TiCl_3$ [143,144]. Other authors have investigated the role of the boron source (SiB_4, FeB, and TiB_2) on the production of $Ca(BH_4)_2$ from the hydrogenation of SiB_4 and CaH_2 [90].

The hydridic–protic interaction has been exploited in a series of RHCs containing borohydride–amide mixtures [145,146]. When the 1:4 molar ratio mixture $Ca(BH_4)_2$-$4LiNH_2$ was ball milled, Equation (32) occurred, leading to the formation of $Ca(NH_2)_2$, $LiBH_4$, and $Li_3(NH_2)_2BH_4$, affording a 26.2% reduction in E_A compared to $LiBH_4$-$2LiNH_2$ chosen as reference [53].

$$Ca(BH_4)_2 + 4\,LiNH_2\ \rightarrow Li_3(NH_2)_2BH_4 + LiBH_4 + Ca(NH_2)_2 \tag{32}$$

Other reports describe a slightly different reaction pathway for the system $Ca(BH_4)_2$-$4LiNH_2$, corresponding to Equation (33) [147]. The formation of mixed anion $Ca(BH_4)(NH_2)_{2-x}$ was also found by Morelle et al. in the RHC system $Ca(BH_4)_{2-x}NaNH_2$ (x = 1, 2, and 3), showing release of NH_3 (300 °C) and H_2 (above 350 °C), and a decreasing decomposition temperature as the amide fraction of the composite increased, which advocates for the destabilization of starting $Ca(BH_4)_2$ by the amide compound ($NaNH_2$) [148].

$$Ca(BH_4)_2 + 4LiNH_2 \rightarrow Li_4BN_3H_{10} + [Ca(BH_4)(NH_2)] \rightarrow \frac{1}{4}LiCa_4(BN_2)_3 + \frac{5}{4}Li_3BN_2 + 8H_2 \tag{33}$$
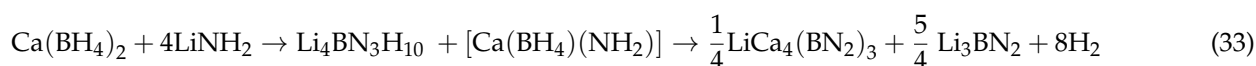
Other molar ratios of $Ca(BH_4)_2$-$xLiNH_2$ have also been investigated, for instance, for x = 3 [149]. The intramolecular destabilization in the systems $Ca(BH_4)_2$-MNH_2 (M=Li, Na) has also been evidenced by Poonyayant et al., when a metathetical reaction led to the formation of cation-mixed, anion-mixed complex hydrides of type $mCa(BH_4)_2(NH_2)$ with a release profile starting at ca. 150 °C through hydridic-protic interactions in a two-step release accounting for 9.3 wt% [98]. The $Mn(BH_4)_2$–CaH_2 mixture system (1:1 molar, manual grinding) led to the more stable $Ca(BH_4)_2$ through a double exchange reaction, which effectively suppressed the formation of diborane in the utilized system [150].

Investigation of the $Ca(BH_4)_2$-2.5 Mg_2NiH_4 RHC was shown to proceed through three different pathways, depending on the hydrogen backpressure, which again highlights the aspects of chemical equilibrium (Equations (34) - 2.3 wt%, (35) - 4.2 wt%, (36) - 4.6 wt%) [151]. At 1 bar, the reaction proceeds via Equation (36), whereas at 20 or 50 bar, all three reactions occur simultaneously.

$$Ca(BH_4)_2 + 2.5\ Mg_2NiH_4 \rightarrow 0.25\ Ca_4Mg_3H_{14} + MgNi_{2.5}B_2 + 3.25\ MgH_2 + 4H_2 \quad (34)$$

$$Ca(BH_4)_2 + 2.5\ Mg_2NiH_4 \rightarrow 0.25\ Ca_4Mg_3H_{14} + MgNi_{2.5}B_2 + 3.25\ Mg + 7.25\ H_2 \quad (35)$$

$$Ca(BH_4)_2 + 2.5\ Mg_2NiH_4 \rightarrow CaH_2 + MgNi_{2.5}B_2 + 4\ Mg + 8\ H_2 \quad (36)$$
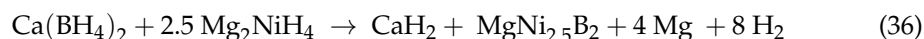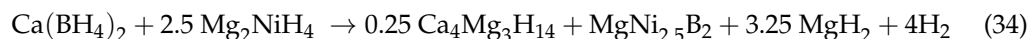
The influence of alkali metal amides on the desorption properties of calcium borohydride was studies by Chu et al. [152], concluding that the driving force of reactions (37) and (38) must lie in the interaction B–H and N–H present in the milled RHC $M(NH_2)_2$–$Ca(BH_4)_2$ (M=Mg, Ca).

$$Ca(BH_4)_2 + 2\ Mg(NH_2)_2 \rightarrow \frac{1}{3}\ [Ca_3Mg_6(BN_2)_6] + 8\ H_2 \quad (37)$$

$$Ca(BH_4)_2 + 2\ Ca(NH_2)_2 \rightarrow \frac{1}{3}\ Ca_9(BN_2)_6 + 8\ H_2 \quad (38)$$
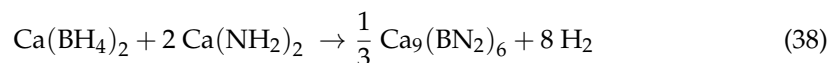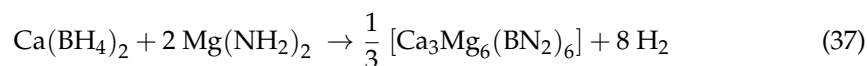
Binary, ternary and quaternary mixtures in the $LiBH_4$-$NaBH_4$-KBH_4-$Mg(BH_4)_2$-$Ca(BH_4)_2$ system have been investigated by Dematteis et al. showing that new phases occurring might originate from the interaction $Mg(BH_4)_2$-$Ca(BH_4)_2$ [153–155]. This interaction in the $Mg(BH_4)_2$-$Ca(BH_4)_2$ was studied in the 5:1 molar ratio showing a destabilization effect of $Ca(BH_4)_2$ over $Mg(BH_4)_2$ [94,95].

Another improvement strategy regarding H_2 storage performance is utilization of eutectic mixture, and 0.68 $LiBH_4$-0.32 $Ca(BH_4)_2$ is a known and tested model system [156,157]. Interestingly, the eutectic mixture of borohydrides can release H_2 below each individual components, and even a release onset below the melting of pristine complex hydride [157]. When used as an additive, $Ca(BH_4)_2$ can produce very notable improvements; $Mg(NH_2)_2$–$2LiH$–$0.1Ca(BH_4)_2$ for instance can release 4.5 wt% H_2 with onset at 90 °C, and a rehydrogenation temperature of 60 °C [131]. The synergistic effect of the formed CaH_2 and $LiBH_4$ probably played a role in the improvement recorded [131]. Li et al. have studied the system $2LiNH_2$–MgH_2–$xCa(BH_4)_2$ with a very low desorption onset of 80 °C and a 8.2 wt% hydrogen storage content (x = 0.3); the system $2LiNH_2$–MgH_2–$0.1Ca(BH_4)_2$ was also studied. [158]. It's worth noting that a tentative metathesis reaction of $NaBH_4$ and $CaCl_3$ did not yield the expected $Ca(BH_4)_2$ product, and il led to $CaNa(BH_4)_{1-x}Cl_x$ instead, which forms as a result of a diffusional process of one reagent into the other [46].

Other additives potentially leading to calcium borohydride have also been employed: $2LiBH_4$–CaH_5 (featuring a lower 1.1 wt% storage capacity at a lower temperature of 270 °C [159]. A combination of different complex hydrides (alanate–borohydride) was proposed by Moller et al., namely, $NaAlH_4$ + $Ca(BH_4)_2$ [160]. This approach led to $NaBH_4$ and $Ca(AlH_4)_2$ through a metathesis reaction, releasing ca. 6 wt% H_2 below 400 °C [160]. The system $NaAlH_4$ + $Ca(BH_4)_2$ has been investigated mechanistically by Mustafa et al., who identified various decomposition intermediates in the multi-step desorption of the RHC, like $CaAlH_5$, Al, CaH_2, Al_4Ca, and Al_2Ca (Figure 10) [135,161].
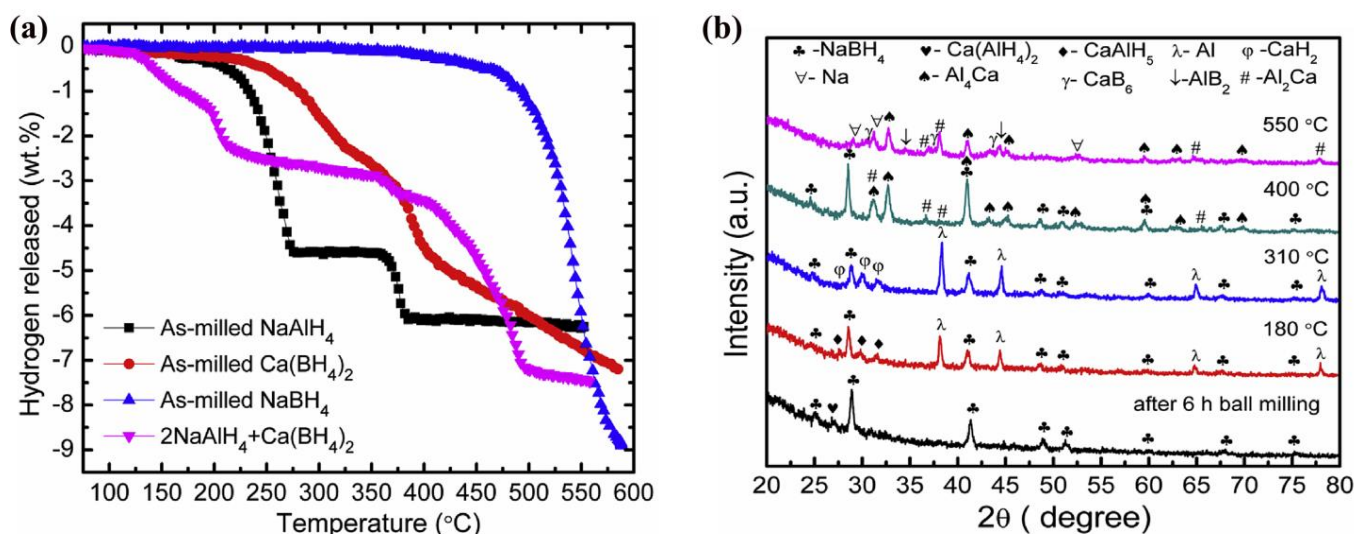
Figure 10. (**a**) TPD curves of the as-milled $NaAlH_4$, as-milled $Ca(BH_4)_2$, as-milled $NaBH_4$, and $2NaAlH_4$ + $Ca(BH_4)_2$; (**b**) XRD patterns of the $2NaAlH_4 + Ca(BH_4)_2$ composite after 6 h of ball milling and after dehydrogenation at 180 °C, 310 °C, 400 °C, and 550 °C. Reprinted with permission from Ref. [161].

The ternary system $Ca(BH_4)_2$–$LiBH_4$–MgH_2 was reported to exhibit long-term cycling stability [162], the precursors CaH_2–MgB_2 thin films allowed identification of individual steps leading to the formation of $Ca(BH_4)_2$ [163], the effect of MgF_2 additive was studied in the system $Ca(BH_4)_2$-MgF_2 with up to 5.8 wt% H_2 uptake at 330 °C after 2.5 h during the first three a/d cycles [125], the formation of β–$Ca(BH_4)_2$ in the γ-$Mg(BH_4)_2$-CaH_2 RHC system [164], $LaMg_3$-catalyzed $Ca(BH_4)_2$–$LiBH_4$ with H_2 release onset at 150 °C and good capacity retention of 70% after five a/d cycles [78], or DFT investigations in the KBH_4–$Ca(BH_4)_2$ system [79].

When MgH_2 is used, destabilization occurs, and a system with a total H_2 capacity of 9.1 wt% is generated (Equation (39)) [165]. This type of reactivity was also proven by Kim et al., who demonstrated the reversibility of the $Ca(BH_4)_2$+MgH_2 RHC, where the formation of CaB_2 boride seems to be essential while the formation of a-B is a major downside [107].

$$Ca(BH_4)_2 + MgH_2 \rightarrow \frac{2}{3} CaH_2 + \frac{1}{3} CaB_6 + Mg + \frac{13}{3} H_2; \ 9.1 \ wt\% \ H_2 \qquad (39)$$
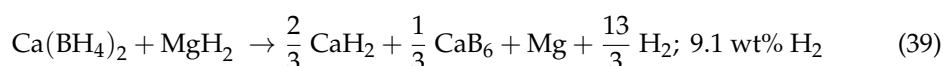
Other RHCs like $LiBH_4$-$Ca(BH_4)_2$ were investigated over a wide compositional domain by Lee et al. in $xLiBH_4$+$(1-x)Ca(BH_4)_2$ ($0 < x < 1$) [166], by Yan et al. in the eutectic composite $LiBH_4$+$Ca(BH_4)_2$ [167], or when nanoconfined in mesoporous scaffolds of type CMK-3 [68,116,118] or SBA-15 as support, with enhanced interface interaction [115]. In fact, combining nanocatalysts (NbF_5) and nanoconfinement (CMK-3 ordered mesoporous carbon) afforded a total capacity of 13.3 wt% for the system $LiBH_4$–$Ca(BH_4)_2$ in the resulting nanocomposite $0.68LiBH_4$–$0.32Ca(BH_4)_2$–$0.05NbF_5$@CMK-3 [118].

$xNaBH_4$-$(1-x)Ca(BH_4)_2$ composite, however, unlike the $Mg(BH_4)_2$ counterpart, yielded no eutectic melting, hence there was no improvement over H_2 release temperature [168]. Employing organic borohydrides, such as guanidinium borohydride (GBH), led to a marked improvement in the $Ca(BH_4)_2$/$C(NH_2)_3]^+[BH_4]^-$ coupled system, which suppressed ammonia release and afforded ca. 10 wt% H_2 evolution between 60 and 300 °C [169].

There have been attempts to increase the stability of $Al(BH_4)_3$ (volatile), and compounding it with $Ca(BH_4)_2$ by Titov et al. was one of them, leading to the formation of the complex $Ca(BH_4)_2 \cdot Al(BH_4)_3$ (slow reaction: 3–4 days) with a postulated structure $[Ca(BH_4)]^+[Al(BH_4)_4^-]$, in line with experimental IR data [24]. Some representative RHCs and their hydrogen storage performance are summarized in Table 3.

Table 3. Hydrogen storage characteristics of RHCs based on $Ca(BH_4)_2$ and its precursors.

Ca-Based Storage Material	Synthesis Method	wt% H_2 Storage Performance	Obs. (Reversibility, Catalyst)	Ref.
$3CaH_2 + 4MgB_2 + CaF_2$	Ball milling in a Spex mill (87 h in total)	7.0 %	$Ca(BH_4)_2$ and MgH_2 formed after hydrogenation; $E_A = 116\ 75$ kJ mol^{-1} H_2 after cycling	[170,171]
$Ca(BH_4)_2 + MgH_2$	Ball milling; TiF_4/NbF_5 catalysts	10.5%	60% reversibility (350 °C, 90 bar H_2)	[165]
$Ca(BH_4)_2$-$3LiNH_2$	Ball milling	7.2%	300 °C, 3 h; desorption onset at 200 °C	[146,149]
$Ca(BH_4)_2$-$4LiNH_2$	Liquid ball milling	8.86 %	NH_3 evolution is restrained	[53]
$Ca(BH_4)_2$-$4LiNH_2$	Ball milling	8% (288 °C)	5 wt% $CoCl_2$ additive lowers onset to 178 °C	[147]
$Ca(BH_4)_2$-$xNaNH_2$ (x = 1,2,3)	Hand grinding	7.5–9% (NH_3 + H_2)	Metathesis at 100–150 °C to $Ca(BH_4)(NH_2)$; NH_3 release (t < 300 °C) and H_2 (t > 350 °C)	[148,161]
$Ca(BH_4)_2$–Mg_2NiH_4	Fritsch Planetary P6 milling	4.6%	Mutual destabilization; formation of $MgNi_{2.5}B_2$	[151]
$Ca(BH_4)_2$–$6Mg_2FeH_6$	Ball milling	-	Desorption onsets at 310 °C (vs. 350 °C for pristine $Ca(BH_4)_2$)	[172]
Mg_2NiH_4-$LiBH_4$-$Ca(BH_4)_2$	Ball milling	-	$MgNi_{2.5}B_2$, Mg, and $Mg_2NiH_{0.3}$ as intermediates	[173]
$Ca(BH_4)_2$–$2Mg(NH_2)_2$ and $Ca(BH_4)_2$–$2Ca(NH_2)_2$	Ball milling (Retsch PM400 planetary ball mill, 200 rpm, 5 h, Ar)	8.3%, resp. 6.8%	Desorption onsets at 220 °C	[152]
$Mg(BH_4)_2$–$Ca(BH_4)_2$ (1:2, 1:1, 2:1)	Fritsch Pulverisette 6 planetary milling	-	Partial reversibility reported only for $2Mg(BH_4)_2$–$Ca(BH_4)_2$	[94,153]
$NaAlH_4$–$Ca(BH_4)_2$	Fritsch Pulverisette 6, WC vials and balls, BPR 40	6%	$Ca(AlH_4)_2$ was partially stable (10 months), yielding Al and CaH_2	[160]
$2NaAlH_4 + Ca(BH_4)_2$ (+5 wt% TiF_3 catalyst)	Ball milling (6 h)	4.1 wt% (at 420 °C)	TiF_3 doping reduced release onset from 125 °C (pristine) to 60 °C; Al_3Ti, CaF_2 intermediates (also catalysts)	[135,161]
$Ca(BH_4)_2$/ $[C(NH_2)_3]^+[BH_4]^-$ (GBH)	Ball milling	10%	Onset at 60 °C, full release below 300 °C (GBH = guanidinium borohydride)	[169]

5.5. Adduct Formation and Dihydrogen Bonding in Solvates

From molecular insights into the dihydrogen bonding in borohydride ammoniates [174] to DFT modeling of chemical bonding [175,176] or the dehydrogenation mechanism in $Ca(BH_4)_2 \cdot 2NH_3$ [177,178], as well as experimental confirmation of the theoretical aspects [179], various adducts of $Ca(BH_4)_2$ have been described and investigated [39,179,180], including calcium tetradecahydroundecaborate $Ca(B_{11}H_{14})_2 \cdot 4Dg$ (Dg = diglyme) [181]. The first ammoniate of calcium borohydride was synthesized and characterized by Chu et al., who isolated it by direct synthesis from components $Ca(BH_4)_2 \cdot 2NH_3$ (space group *Pbcn*) featuring longer B–H and N–H bond lengths due to dihydrogen bonding, which facilitates the release of 11.3 wt% H_2 at 250 °C [182]. DFT studies performed on $Ca(BH_4)_2 \cdot 2NH_3$ reveal that the Ea of 1.41 eV for thermal decomposition can be tuned by using metal dopants (Fe, Co, and Ni) that can modify the Fermi level [183]. While the adduct $Ca(BH_4)_2 \cdot NH_3$ typically releases NH_3 upon heating at 162–250 °C, when a multi-cation strategy was employed by Tang et al., the RHC $Ca(BH_4)_2 \cdot NH_3$/$LiBH_4$ released 12 wt% H_2 of high purity (>99%) at 250 °C [184]. The reaction leading to such a behavior was a two-step process described by Equation (40) [184].

$$Ca(BH_4)_2 \cdot NH_3 + LiBH_4 \xrightarrow{-3H_2} [LiCaNB_3H_9] \xrightarrow{-\frac{7}{2}H_2} \frac{1}{4}[Li_4B_{10}H_6] + \frac{1}{4}Ca_3B_2N_4 + \frac{1}{4}CaH_2 \qquad (40)$$
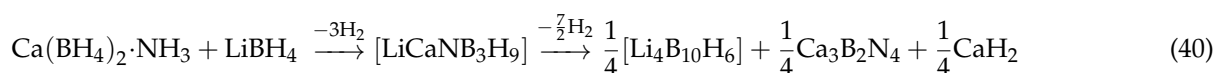
Furthermore, the addition of $Mg(BH_4)_2$ over $Ca(BH_4)_2 \cdot nNH_3$ (n = 1, 2, 4) revealed an increase in H_2 purity and storage capacity in the system $Ca(BH_4)_2 \cdot 4NH_3$–$Mg(BH_4)_2$, a

synergy that inhibited ammonia release to yield >99% pure H_2 upon thermal treatment at 500 °C [179].

Extending the scope of borohydride adducts of calcium borohydride, Li et al. studied the hydrogen release properties of calcium borohydride hydrazinates $Ca(BH_4)_2.nN_2H_4$ (n = 1, 4/3, 2, 3). Among these compounds, the monohydrazinate $Ca(BH_4)_2.4/3$ N_2H_4 showed 10.8 wt% H_2 release with a dehydrogenation temperature of 140 °C when utilizing an Fe-based catalyst (2 wt% $FeCl_3$) [185].

Other complexes have also been reported, such as the AB (ammonia borane) adducts of complex hydrides, mainly $Ca(BH_4)_2(NH_3BH_3)_2$ and its lithium counterpart [186]. The AB adduct of calcium borohydride showed partially reversible behavior (2.4 wt%) under moderate conditions (82 bar H_2, 400 °C), with a release of 11 wt% H_2. Guadinate adducts of metal borohydrides have been reported by Wu et al. in the case of Li, Mg, and Ca complex hydrides $MBH_4 \cdot nCN_3H_5$ [187]. The low contamination of gaseous decomposition products with ammonia and diborane was based on the C–N bonds of guanidine and H^- anion of borohydrides. $Ca(BH_4)_2 \cdot 2CN_3H_5$ released about 10 wt% H_2 under modest conditions [187].

5.6. Reversibility Assessment

As a key element in advancing hydrogen storage materials, reversibility remains one of the toughest problems in solid-state energy storage [11,104,188–190]. The influence that metal fluorides exert on $Ca(BH_4)_2$ dehydrogenation/rehydrogenation was studied in the case of VF_4, TiF_4, and NbF_5 [133]. Several systems were investigated and showed various degrees of reversibility, such as pristine [191] and TiF_4- and NbF_5–catalyzed $Ca(BH_4)_2$–MgH_2 [132], $Ca(BH_4)_2$–Mg_2NiH_4 [151,192], $LiBH_4$–$Ca(BH_4)_2$ [166], ternary RHCs with higher reversibility $Ca(BH_4)_2$–$LiBH_4$–MgH_2 [162], $Ca(BH_4)_2$–MgF_2 [125], the implications of $CaB_{12}H_{12}$ on cycling capacity of calcium-based RHCs [41,193–195], eutectic mixture $LiBH_4$–$Ca(BH_4)_2$ [156], the use of catalyst ($TiCl_3$ [196]; TiF_3, NbF_5, $NbCl_5$ [197]) on the reversibility of $Ca(BH_4)_2$ (rehydrogenation under 90 bar H_2, 623 K, 3.8 wt% H_2) [196].

The catalytic effect of $Ca(BH_4)_2$ was explored in a RHC $Mg(NH_2)_2$–$2LiH$–$0.1Ca(BH_4)_2$ composite (4.5 wt% H_2 reversible, onset at 90 °C and release at 140 °C, and rehydrogenation with onset at 60 °C) [131]. Other RHCs serve as precursors for calcium borohydride, and these systems already showed promising results regarding cycling behavior, like $LiBH_4$–$Ca(AlH_4)_2$ (4.5 wt% reversible, 450 °C) [198]. TiX_3 (X=F, Cl) has been successfully used to lower the thermodynamic barriers of $Ca(BH_4)_2$ [138] or in RHCs $6LiBH_4$–CaH_2 systems [143]. A critical step for the reversibility of $Ca(BH_4)_2$ is the formation of CaB_6, presumably from a CaB_2H_6 precursor that can only be produced between 320 and 350 °C; otherwise, amorphous B would result, which is a clear bottleneck in the cycling pathway of calcium borohydride [104,199].

5.7. Ionic Conductivity

Ionic conductivity [173,200–207] and superconductivity [208,209] have also been investigated recently, with some surprising results and direct implications in the applicability of $Ca(BH_4)_2$ in electrolytes for batteries or even as high-temperature superconductors when properly doped, as DFT computations have revealed.

It has been hypothesized that Ca^{2+} might be too big for migration in Ca-based electrolytes, preferring an octahedral coordination by binding six ligands, but recent reports imply that using weaker coordinating ligands, such as $B_{12}H_{12}^{2-}$ might increase Ca^{2+} mobility.

6. Ca(BH₄)₂ in Organic Synthesis and Organometallic Chemistry

6.1. Catalyst/Initiator

Calcium borohydride extends its utility in organic synthesis as well. For instance, the THF adduct $[Ca(BH_4)_2(THF)_2]$ was prepared from $Ca(oMe)_2$ and $BH_3.THF$ reacting in THF solvent and used for the polymerization ε-caprolactone and L-lactide in a combined DFT and experimental investigation [210]. The active catalysts employed

were produced by the treatment of [Ca(BH$_4$)$_2$(THF)$_2$] with KCp* (Cp* = (η^5-C$_5$Me$_5$)) and K{(Me$_3$SiNPPh$_2$)$_2$CH}, namely producing dimeric heteroleptic mono-borohydride derivatives [Cp*Ca(BH$_4$)(THF)$_n$]$_2$ and [{(Me$_3$SiNPPh$_2$)$_2$CH}Ca(BH$_4$)(THF)$_2$] (Figure 11). These heteroleptic borohydrides were used as initiators for the ring-opening polymerization (ROP) of ε-caprolactone and L-lactide in good yields [210].
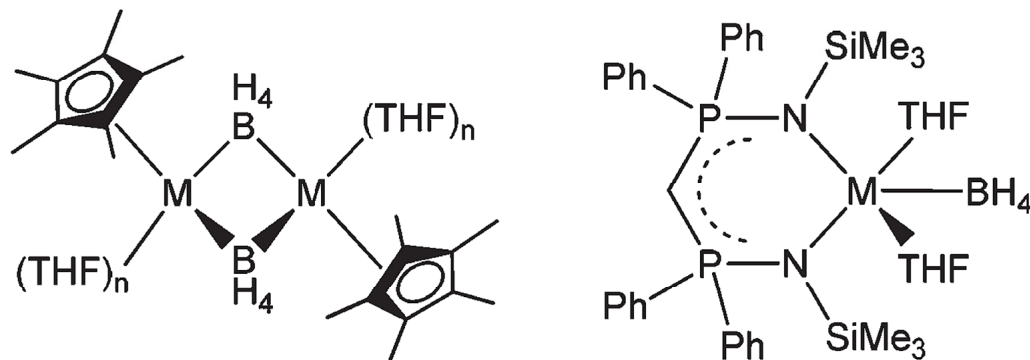
Figure 11. Ca-based (M=Ca) borohydride complexes used for ROP reactions [210].

6.2. Reducing Agent

Borohydride compounds can typically be used for reduction reactions, given their [BH$_4$]$^-$ anion-reducing characteristics. For example, Ca(BH$_4$)$_2$ afforded the reduction of the corresponding organic precursor to β-vanillyl-γ-butyrolactone [211] (Figure 12).
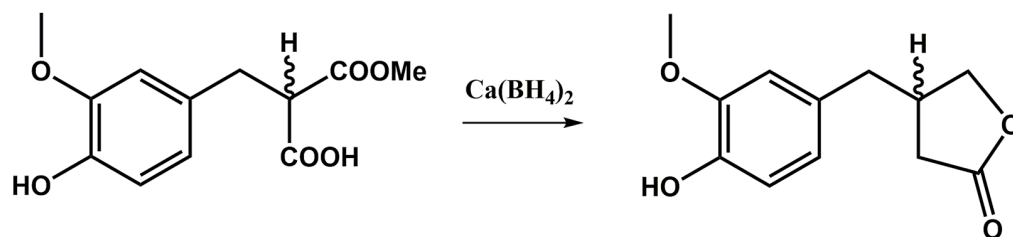
Figure 12. Chemical reduction of organic esters and acids performed by calcium borohydride [211].

The reduction of β–keto esters was also shown to be effective when using Ca(BH$_4$)$_2$, yielding corresponding hydroxy-acids and, further on, water elimination to yield α, β—unsaturated acids [212]. Aliphatic and aromatic esters R(Ar)COOEt were fully reduced to alcohols E(Ar)CH$_2$OH by Ca(BH$_4$)$_2$ in the presence of alkene catalysts such as 1-decene, cyclohexene [213,214], or cyclooctadiene (COD) [215].

A sulfurated modified calcium borohydride complex, Ca(BH$_2$S$_3$)$_2$, was synthesized and used for the reduction of aryl azides and aryl nitro derivatives to their corresponding Ar-NH$_2$ amino compounds when refluxed in THF, resulting in high yields [216]. The synthesis of Ca(BH$_2$S$_3$)$_2$ proceeds via a metathetical reaction of NaBH$_2$S$_3$ and CaCl$_2$ in THF, the driving force being the higher stability of the calcium-sulfurated borohydride compared to the sodium counterpart, which undergoes decomposition when exposed to air and moisture (Equation (41)) [216]. Additionally, Ca(BH$_2$S$_3$)$_2$ can easily reduce carbonyl compounds (aldehydes, ketones, acyloins, α-diketones, α, β—unsaturated carbonyl compounds, azides, and carboxylic acid chlorides) to their corresponding alcohols in high yields [217].

$$NaBH_4 + 3S \xrightarrow{-H_2} NaBH_2S_3 \xrightarrow{\frac{1}{2}\ CaCl_2} \frac{1}{2}\ Ca(BH_2S_3)_2 + NaCl \qquad (41)$$
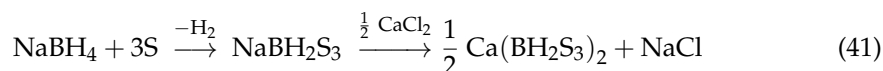
With a lower reactivity towards esters compared to lithium borohydride, Ca(BH$_4$)$_2$ was used together with Grignard reagents in a molar ratio of 0.25 Ca(BH$_4$)$_2$:4 EtMgBr to produce the reduction of methyl esters RCOOMe in THF at room temperature to RCH$_2$OH

alcohol (6%), RCH(OH)Et (83%), and RC(OH)Et$_2$ (11%) [218]. Both Ca(BH$_4$)$_2$ and Zn(BH$_4$)$_2$ were investigated in this reduction and showed similar results.

Another modified borohydride complex, calcium amidoborane Ca(NH$_2$BH$_3$)$_2$ was used successfully to reduce α, β–unsaturated aldehydes and ketones (carbonyl compounds) to allylic alcohols [219]. Its synthesis involves the reaction of CaH$_2$ and AB (ammonia borane) in THF (Equation (42)) [219].

$$CaH_2 + 2\,NH_3BH_3 \xrightarrow{\text{THF}} Ca(NH_2BH_3)_2 + 2H_2 \tag{42}$$
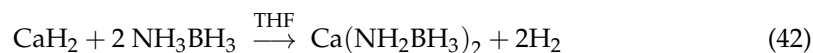
6.3. Promoter of Cyclization in Various Reactions

Calcium borohydride was also involved as an active catalyst in σ-bond metathesis, a fundamental reaction in organic chemistry [220]. Notably, Bellham et al. reacted amine-borane t-BuNH$_2$·BH$_3$ with a β-diketiminate-supported silylamido calcium complex with elimination of HN(SiMe$_3$)$_2$ while also isolating the active catalyst, characterized by XRD and shown to belong to a polymeric infinite chain of calcium borohydride, in soluble in organic media, namely, [Ca(BH$_4$)$_2$·THF]$_\infty$ [221]. Access to polylactide macrocycles by cyclo-polymerization of L-lactide was reported to proceed in good yield (up to 77%, 20 min) when catalyzed by Ca(BH$_4$)$_2$ by intramolecular transesterification occurring during ROP [222–224].

6.4. Reaction Inhibitor and Miscellaneous Reactivity

There are reports of other derivatives of calcium borohydride, like the cyclopentadienyl complex Cp$_2$Ca(THF)$_2$ (obtained by mixing Ca(BH$_4$)$_2$ and CpNa in THF) and the methyl-substituted analog, (MeCp)$_2$Ca(THF)$_2$ (MeCp = η^S-CH$_3$C$_5$H$_4$) [225]. Similarly, [Bm$^{\text{MeBenz}}$]$_2$Ca(THF)$_2$ was also obtained and characterized by the reaction of Ca(BH$_4$)$_2$·2THF with 1-methyl-1,3-dihydro-2H-benzimidazole-2-thione, where Ca is eight-coordinate and features two Ca . . . H-B interactions [226].

Ca(BH$_4$)$_2$ has served as the starting point for the synthesis of thorium and uranium metallocene borohydride complexes, allowing the isolation and structure determination of (C$_5$Me$_5$)$_2$Th(η^3-H$_3$BH)$_2$ [227].

Alternatively, calcium borohydride found its use as an inhibitor for the synthesis of fluorine-modified polysilazanes, leading to a solid, soluble fluorinated polysilazane suitable for metal substrates coating [228], or as a catalyst for regioselective hydroboration of terminal alkenes [214].

7. Remaining Challenges and Future Prospects

While bearing some similarities to its lighter counterpart Mg(BH$_4$)$_2$, calcium borohydride features some unique features like the relative ease of desolvation from synthesis adducts, different de-/rehydrogenation enthalpies, a lower and thus more feasible activation energy E$_a$, and different decomposition pathways. This decomposition could be further tuned, allowing the generation of high-purity hydrogen with small amounts of boranes.

The use of calcium borohydride as an energy storage material has the potential to impact the environment in several ways. It is essential to consider both the potential benefits and the hazards associated with the production, handling, and disposal of this complex hydride and its related composites. Regarding the production route, hazardous chemicals are involved in the synthesis of calcium borohydride as well as energy-intensive processes such as ball milling. These processes may involve the use of solvents, reagents, and catalysts that could have adverse effects on human health and the environment if not properly handled and managed. The production of calcium borohydride requires significant energy inputs, which, depending on the energy source, could contribute to greenhouse gas emissions. Handling complex hydrides involves some strict safety precautions needed to prevent accidental exposure and ensure safety. It is important to follow established safety protocols to minimize risks during transportation, storage, and usage of Ca(BH$_4$)$_2$. Being reactive towards moisture with the subsequent release of hydrogen gas, calcium

borohydride can be flammable and potentially lead to fire or explosion hazards; therefore, adequate measures must be taken to prevent accidental ignition and control the release of hydrogen gas.

An important aspect linked to the circular economy and a sustainable hydrogen economy is the disposal of end-of-life hydrogen storage materials based on $Ca(BH_4)_2$. Since a reaction with water would lead to the release of hydrogen, proper disposal methods should be followed to ensure the safe handling of any H_2 generated during disposal processes. The impact associated with the disposal of calcium borohydride waste, if not properly managed, could be linked to adverse environmental effects. It is important to adhere to local regulations and guidelines for the disposal of hazardous waste to prevent contamination of soil, water, or air. Furthermore, the overall environmental impact of calcium borohydride as an energy storage material can be evaluated by life cycle assessment studies that consider the potential environmental impact throughout the entire life cycle of the compound, including production, usage, and disposal, and could guide the development of more sustainable processes.

Reversibility perhaps remains the highest barrier to adopting $Ca(BH_4)_2$ as a mainstream hydrogen storage fuel, along with the currently rather cumbersome synthesis procedure. The formation of various rock-stable boron by-products (CaB_6, for instance) or other very stable compounds still represents important research avenues to explore. The multistep decomposition can be altered by using catalysts/additives or by conducting the reaction in a suitable solvent capable of decreasing reaction enthalpies by forming borohydride adducts. Among TM-based catalysts, Nb and Ti showed the best results, lowering rehydrogenation conditions (350 °C, 24 h, 90 bar H_2). These results add to other reports where nanoconfined $Ca(BH_4)_2$ in various nanosized supports, such as carbonaceous hosts [229], achieved a reliable H_2 storage capacity, although much lower than the theoretical one.

Additionally, research efforts should focus on developing environmentally friendly synthesis routes, optimizing energy consumption during production, and exploring recycling methods for calcium borohydride waste. Adherence to regulations, responsible waste management, and continuous improvement in production and disposal practices are essential to minimizing the environmental footprint of calcium borohydride and ensuring its safe and sustainable use.

8. Conclusions

With a high production cost, calcium borohydride sits in an awkward place among solid-state hydrogen storage materials; it offers nearly 10 wt% H_2 storage but with restricted reversibility and sluggish kinetics, which require the use of catalysts and potentially novel additives. Nanostructuring may be another avenue for researchers to follow in order to achieve improved behavior of $Ca(BH_4)_2$ during hydrogenation studies. Calcium borohydride $Ca(BH_4)_2$ remains one of the most promising tetrahydridoborates due to its high hydrogen storage capacity, the relative abundance of starting raw materials, and its pivotal role in catalysis for many decades.

The current study has highlighted the synthesis routes for $Ca(BH_4)_2$, the identified polymorphs, and various adducts that could potentially yield high-capacity hydrogen storage systems while also significantly reducing production costs. Catalyst/additive compounding is another route to improving a/d kinetics, together with nanosizing and/or nanoconfinement. The wide range of applications of $Ca(BH_4)_2$, from energy storage systems to batteries, organic synthesis, organometallic chemistry, and catalysis, have been reviewed.

Understanding the key steps and intermediates of the decomposition pathways of $Ca(BH_4)_2$ under different experimental conditions could allow further advances by tuning the thermodynamics and kinetics of hydrogen release/uptake. Other strategies focused on using RHCs containing $Ca(BH_4)_2$, while species containing $B_{12}H_{12}^{2-}$ anion might be suitable in ion conductivity studies. Addressing the challenges related to synthesis methods, reaction mechanisms, hydrogen release kinetics, and overall device performance

is essential for realizing its full potential. Further research is needed to bridge the existing knowledge gaps and unlock the practical applications of calcium borohydride in energy storage systems. Additionally, several reports of using $Ca(BH_4)_2$ in catalysis and organic synthesis as a reductant reaffirm the advantages of the plurivalent calcium borohydride.

Conflicts of Interest: The author declares no conflict of interest. The funders had no role in the design of the study; in the collection, analyses, or interpretation of data; in the writing of the manuscript; or in the decision to publish the results.

References

1. Amieiro-Fonseca, A.; Ellis, S.R.; Nuttall, C.J.; Hayden, B.E.; Guerin, S.; Purdy, G.; Soulié, J.-P.; Callear, S.K.; Culligan, S.D.; David, W.I.F.; et al. A multidisciplinary combinatorial approach for tuning promising hydrogen storage materials towards automotive applications. *Faraday Discuss.* **2011**, *151*, 369–384. [CrossRef] [PubMed]
2. Comanescu, C. Recent Development in Nanoconfined Hydrides for Energy Storage. *Int. J. Mol. Sci.* **2022**, *23*, 7111. [CrossRef] [PubMed]
3. Bonaccorsi, R.; Charkin, O.P.; Tomasi, J. Nonempirical study of the structure and stability of beryllium, magnesium, and calcium borohydrides. *Inorg. Chem.* **1991**, *30*, 2964–2969. [CrossRef]
4. Comanescu, C. Complex Metal Borohydrides: From Laboratory Oddities to Prime Candidates in Energy Storage Applications. *Materials* **2022**, *15*, 2286. [CrossRef]
5. Grinderslev, J.B.; Amdisen, M.B.; Skov, L.N.; Moller, K.T.; Kristensen, L.G.; Polanski, M.; Heere, M.; Jensen, T.R. New perspectives of functional metal borohydrides. *J. Alloys Compd.* **2022**, *896*, 163014. [CrossRef]
6. Comanescu, C. Paving the Way to the Fuel of the Future—Nanostructured Complex Hydrides. *Int. J. Mol. Sci.* **2023**, *24*, 143. [CrossRef]
7. Kojima, Y. Hydrogen storage materials for hydrogen and energy carriers. *Int. J. Hydrogen Energy* **2019**, *44*, 18179–18192. [CrossRef]
8. Nakamori, Y.; Li, H.W.; Matsuo, M.; Miwa, K.; Towata, S.; Orimo, S. Development of metal borohydrides for hydrogen storage. *J. Phys. Chem. Solids* **2008**, *69*, 2292–2296. [CrossRef]
9. Ronnebro, E. High-pressure techniques for discovering and re-hydrogenation of metal hydride materials. *J. Phys. Chem. Solids* **2010**, *71*, 1154–1158. [CrossRef]
10. Ronnebro, E. Development of group II borohydrides as hydrogen storage materials. *Curr. Opin. Solid State Mater. Sci.* **2011**, *15*, 44–51. [CrossRef]
11. Ronnebro, E.; Majzoub, E.H. Calcium borohydride for hydrogen storage: Catalysis and reversibility. *J. Phys. Chem. B* **2007**, *111*, 12045–12047. [CrossRef] [PubMed]
12. Wolverton, C.; Siegel, D.J.; Akbarzadeh, A.R.; Ozolins, V. Discovery of novel hydrogen storage materials: An atomic scale computational approach. *J. Phys.-Condens. Matter* **2008**, *20*, 064228. [CrossRef] [PubMed]
13. Barkhordarian, G.; Jensen, T.R.; Doppiu, S.; Bosenberg, U.; Borgschulte, A.; Gremaud, R.; Cerenius, Y.; Dornheim, M.; Klassen, T.; Bormann, R. Formation of $Ca(BH_4)_2$ from hydrogenation of CaH_2 + MgB_2 composite. *J. Phys. Chem. C* **2008**, *112*, 2743–2749. [CrossRef]
14. He, L.Q.; Li, H.W.; Tumanov, N.; Filinchuk, Y.; Akiba, E. Facile synthesis of anhydrous alkaline earth metal dodecaborates $MB_{12}H_{12}$ (M = Mg, Ca) from $M(BH_4)_2$. *Dalton Trans.* **2015**, *44*, 15882–15887. [CrossRef]
15. Jepsen, L.H.; Lee, Y.S.; Cerny, R.; Sarusie, R.S.; Cho, Y.W.; Besenbacher, F.; Jensen, T.R. Ammine Calcium and Strontium Borohydrides: Syntheses, Structures, and Properties. *Chemsuschem* **2015**, *8*, 3472–3482. [CrossRef]
16. Karabulut, A.F.; Guru, M.; Boynuegri, T.A.; Aydin, M.Y. Synthesis of $Ca(BH_4)_2$ from Synthetic Colemanite Used in Hydrogen Storage by Mechanochemical Reaction. *J. Electron. Mater.* **2016**, *45*, 3957–3963. [CrossRef]
17. Lee, Y.S.; Filinchuk, Y.; Lee, H.S.; Suh, J.Y.; Kim, J.W.; Yu, J.S.; Cho, Y.W. On the Formation and the Structure of the First Bimetallic Borohydride Borate, $LiCa_3(BH_4)(BO_3)_2$. *J. Phys. Chem. C* **2011**, *115*, 10298–10304. [CrossRef]
18. Titov, L.V. The synthesis of calcium borohydride. *Dokl. Akad. Nauk* **1964**, *154*, 654–656.
19. Titov, L.V. Synthesis and chemical transformations of ionic octahydrotriborates: Cleavage of the B_3H_8-anion. *Russ. J. Inorg. Chem.* **2003**, *48*, 1471–1479.

20. Richter, B.; Grinderslev, J.B.; Moller, K.T.; Paskevicius, M.; Jensen, T.R. From Metal Hydrides to Metal Borohydrides. *Inorg. Chem.* **2018**, *57*, 10768–10780. [CrossRef]

21. Moller, K.T.; Fogh, A.S.; Paskevicius, M.; Skibsted, J.; Jensen, T.R. Metal borohydride formation from aluminium boride and metal hydrides. *Phys. Chem. Chem. Phys.* **2016**, *18*, 27545–27553. [CrossRef] [PubMed]

22. Nakagawa, T.; Ichikawa, T.; Miyaoka, H.; Tsubota, M.; Kojima, Y. Synthesis of Calcium Borohydride by Milling Hydrogenation of Hydride and Boride. *J. Jpn. Inst. Met. Mater.* **2013**, *77*, 609–614. [CrossRef]

23. Rongeat, C.; Lindemann, I.; Borgschulte, A.; Schultz, L.; Gutfleisch, O. Effect of the presence of chlorides on the synthesis and decomposition of Ca(BH$_4$)$_2$. *Int. J. Hydrogen Energy* **2011**, *36*, 247–253. [CrossRef]

24. Titov, L.V.; Eremin, E.R. Complex of aluminum borohydride with calcium borohydride. *Bull. Acad. Sci. Ussr Div. Chem. Sci.* **1975**, *24*, 1095–1096. [CrossRef]

25. George, L.; Saxena, S.K. Structural stability of metal hydrides, alanates and borohydrides of alkali and alkali-earth elements: A review. *Int. J. Hydrogen Energy* **2010**, *35*, 5454–5470. [CrossRef]

26. Karimi, F.; Pranzas, P.K.; Hoell, A.; Vainio, U.; Welter, E.; Raghuwanshi, V.S.; Pistidda, C.; Dornheim, M.; Klassen, T.; Schreyer, A. Structural analysis of calcium reactive hydride composite for solid state hydrogen storage. *J. Appl. Crystallogr.* **2014**, *47*, 67–75. [CrossRef]

27. Llamas-Jansa, I.; Friedrichs, O.; Fichtner, M.; Bardaji, E.G.; Zuttel, A.; Hauback, B.C. The Role of Ca(BH$_4$)$_2$ Polymorphs. *J. Phys. Chem. C* **2012**, *116*, 13472–13479. [CrossRef]

28. Sharma, M.; Sethio, D.; D'Anna, V.; Fallas, J.C.; Schouwink, P.; Cerny, R.; Hagemann, H. Isotope Exchange Reactions in Ca(BH$_4$)$_2$. *J. Phys. Chem. C* **2015**, *119*, 29–32. [CrossRef]

29. Soloninin, A.V.; Babanova, O.A.; Skripov, A.V.; Hagemann, H.; Richter, B.; Jensen, T.R.; Filinchuk, Y. NMR Study of Reorientational Motion in Alkaline-Earth Borohydrides: Beta and gamma Phases of Mg(BH$_4$)$_2$ and alpha and beta Phases of Ca(BH$_4$)$_2$. *J. Phys. Chem. C* **2012**, *116*, 4913–4920. [CrossRef]

30. Buchter, F.; Lodziana, Z.; Remhof, A.; Friedrichs, O.; Borgschulte, A.; Mauron, P.; Zuttel, A.; Sheptyakov, D.; Palatinus, L.; Chlopek, K.; et al. Structure of the Orthorhombic gamma-Phase and Phase Transitions of Ca(BD$_4$)$_2$. *J. Phys. Chem. C* **2009**, *113*, 17223–17230. [CrossRef]

31. Noritake, T.; Aoki, M.; Matsumoto, M.; Miwa, K.; Towata, S.; Li, H.W.; Orimo, S. Crystal structure and charge density analysis of Ca(BH$_4$)$_2$. *J. Alloys Compd.* **2010**, *491*, 57–62. [CrossRef]

32. Le, T.; Do, P.M. The Preferable *F2dd* Phase for Ca(BH$_4$)$_2$ Crystal Under Hydrostatic Pressures. *J. Electron. Mater.* **2017**, *46*, 3479–3483. [CrossRef]

33. Lee, Y.S.; Kim, Y.; Cho, Y.W.; Shapiro, D.; Wolverton, C.; Ozolins, V. Crystal structure and phonon instability of high-temperature β-Ca(BH$_4$)$_2$. *Phys. Rev. B* **2009**, *79*, 9. [CrossRef]

34. Frankcombe, T.J. Calcium Borohydride for Hydrogen Storage: A Computational Study of Ca(BH$_4$)$_2$ Crystal Structures and the CaB$_2$H$_x$ Intermediate. *J. Phys. Chem. C* **2010**, *114*, 9503–9509. [CrossRef]

35. Filinchuk, Y.; Ronnebro, E.; Chandra, D. Crystal structures and phase transformations in Ca(BH$_4$)$_2$. *Acta Mater.* **2009**, *57*, 732–738. [CrossRef]

36. Majzoub, E.H.; Ronnebro, E. Crystal Structures of Calcium Borohydride: Theory and Experiment. *J. Phys. Chem. C* **2009**, *113*, 3352–3358. [CrossRef]

37. Stavila, V.; Her, J.H.; Zhou, W.; Hwang, S.J.; Kim, C.; Ottley, L.A.M.; Udovic, T.J. Probing the structure, stability and hydrogen storage properties of calcium dodecahydro-closo-dodecaborate. *J. Solid State Chem.* **2010**, *183*, 1133–1140. [CrossRef]

38. Liu, A.; Xie, S.T.; Dabiran-Zohoory, S.; Song, Y. High-Pressure Structures and Transformations of Calcium Borohydride Probed by Combined Raman and Infrared Spectroscopies. *J. Phys. Chem. C* **2010**, *114*, 11635–11642. [CrossRef]

39. Paolone, A.; Palumbo, O.; Rispoli, P.; Miriametro, A.; Cantelli, R.; Luedtke, A.; Ronnebro, E.; Chandra, D. Structural phase transitions and adduct release in calcium borohydride. *J. Alloys Compd.* **2011**, *509*, S691–S693. [CrossRef]

40. Li, X.; Huang, Y.P.; Wei, S.L.; Zhou, D.; Wang, Y.C.; Wang, X.; Li, F.F.; Zhou, Q.; Liu, B.B.; Huang, X.L.; et al. New Phase of Ca(BH$_4$)$_2$ at Near Ambient Conditions. *J. Phys. Chem. C* **2018**, *122*, 14272–14276. [CrossRef]

41. Grahame, A.; Aguey-Zinsou, K.-F. Properties and Applications of Metal (M) dodecahydro-*closo*-dodecaborates (M$_{n=1,2}$B$_{12}$H$_{12}$) and Their Implications for Reversible Hydrogen Storage in the Borohydrides. *Inorganics* **2018**, *6*, 106. [CrossRef]

42. Riktor, M.D.; Filinchuk, Y.; Vajeeston, P.; Bardaji, E.G.; Fichtner, M.; Fjellvag, H.; Sorby, M.H.; Hauback, B.C. The crystal structure of the first borohydride borate, Ca$_3$(BD$_4$)$_3$(BO$_3$). *J. Mater. Chem.* **2011**, *21*, 7188–7193. [CrossRef]

43. Fang, Z.Z.; Kang, X.D.; Luo, J.H.; Wang, P.; Li, H.W.; Orimo, S. Formation and Hydrogen Storage Properties of Dual-Cation (Li, Ca) Borohydride. *J. Phys. Chem. C* **2010**, *114*, 22736–22741. [CrossRef]

44. Jiang, K.; Xiao, X.Z.; Deng, S.S.; Zhang, M.; Li, S.Q.; Ge, H.W.; Chen, L.X. A Novel Li-Ca-B-H Complex Borohydride: Its Synthesis and Hydrogen Storage Properties. *J. Phys. Chem. C* **2011**, *115*, 19986–19993. [CrossRef]

45. Lang, C.G.; Jia, Y.; Liu, J.W.; Wang, H.; Ouyang, L.Z.; Zhu, M.; Yao, X.D. Dehydrogenation and reaction pathway of Perovskite-Type NH$_4$Ca(BH$_4$)$_3$. *Prog. Nat. Sci.* **2018**, *28*, 194–199. [CrossRef]

46. Mattox, T.M.; Bolek, G.; Pham, A.L.; Kunz, M.; Liu, Y.S.; Fakra, S.C.; Gordon, M.P.; Doran, A.; Guo, J.H.; Urban, J.J. Calcium chloride substitution in sodium borohydride. *J. Solid State Chem.* **2020**, *290*, 121499. [CrossRef]

47. Schouwink, P.; Morelle, F.; Sadikin, Y.; Filinchuk, Y.; Cerny, R. Increasing Hydrogen Density with the Cation-Anion Pair BH$_4^-$-NH$_4^+$ in Perovskite-Type NH$_4$Ca(BH$_4$)$_3$. *Energies* **2015**, *8*, 8286–8299. [CrossRef]

48. Grove, H.; Rude, L.H.; Jensen, T.R.; Corno, M.; Ugliengo, P.; Baricco, M.; Sorby, M.H.; Hauback, B.C. Halide substitution in Ca(BH$_4$)$_2$. *Rsc Adv.* **2014**, *4*, 4736–4742. [CrossRef]

49. Rude, L.H.; Filinchuk, Y.; Sorby, M.H.; Hauback, B.C.; Besenbacher, F.; Jensen, T.R. Anion Substitution in Ca(BH$_4$)$_2$-CaI$_2$: Synthesis, Structure and Stability of Three New Compounds. *J. Phys. Chem. C* **2011**, *115*, 7768–7777. [CrossRef]

50. Aeberhard, P.C.; Refson, K.; Edwards, P.P.; David, W.I.F. High-pressure crystal structure prediction of calcium borohydride using density functional theory. *Phys. Rev. B* **2011**, *83*, 174102. [CrossRef]

51. Aidhy, D.S.; Zhang, Y.S.; Wolverton, C. Prediction of a Ca(BH$_4$)(NH$_2$) quaternary hydrogen storage compound from first-principles calculations. *Phys. Rev. B* **2011**, *84*, 134103. [CrossRef]

52. Albanese, E.; Corno, M.; Baricco, M.; Civalleri, B. Simulation of nanosizing effects in the decomposition of Ca(BH$_4$)$_2$ through atomistic thin film models. *Res. Chem. Intermed.* **2021**, *47*, 345–356. [CrossRef]

53. Bai, Y.; Pei, Z.W.; Wu, F.; Wu, C. Role of Metal Electronegativity in the Dehydrogenation Thermodynamics and Kinetics of Composite Metal Borohydride-LiNH$_2$ Hydrogen Storage Materials. *ACS Appl. Mater. Interfaces* **2018**, *10*, 9514–9521. [CrossRef] [PubMed]

54. Blanchard, D.; Riktor, M.D.; Maronsson, J.B.; Jacobsen, H.S.; Kehres, J.; Sveinbjornsson, D.; Bardaji, E.G.; Leon, A.; Juranyi, F.; Wuttke, J.; et al. Hydrogen Rotational and Translational Diffusion in Calcium Borohydride from Quasielastic Neutron Scattering and DFT Calculations. *J. Phys. Chem. C* **2010**, *114*, 20249–20257. [CrossRef]

55. Franco, F.; Baricco, M.; Chierotti, M.R.; Gobetto, R.; Nervi, C. Coupling Solid-State NMR with GIPAW ab Initio Calculations in Metal Hydrides and Borohydrides. *J. Phys. Chem. C* **2013**, *117*, 9991–9998. [CrossRef]

56. Borgschulte, A.; Gremaud, R.; Zuttel, A.; Martelli, P.; Remhof, A.; Ramirez-Cuesta, A.J.; Refson, K.; Bardaji, E.G.; Lohstroh, W.; Fichtner, M.; et al. Experimental evidence of librational vibrations determining the stability of calcium borohydride. *Phys. Rev. B* **2011**, *83*, 024102. [CrossRef]

57. Bosenberg, U.; Pistidda, C.; Tolkiehn, M.; Busch, N.; Saldan, I.; Suarez-Alcantara, K.; Arendarska, A.; Klassen, T.; Dornheim, M. Characterization of metal hydrides by in-situ XRD. *Int. J. Hydrogen Energy* **2014**, *39*, 9899–9903. [CrossRef]

58. Riktor, M.D.; Sorby, M.H.; Chlopek, K.; Fichtner, M.; Buchter, F.; Zuettel, A.; Hauback, B.C. In situ synchrotron diffraction studies of phase transitions and thermal decomposition of Mg(BH$_4$)$_2$ and Ca(BH$_4$)$_2$. *J. Mater. Chem.* **2007**, *17*, 4939–4942. [CrossRef]

59. Suarez-Alcantara, K.; Sorby, M.H.; Pistidda, C.; Karimi, F.; Saldan, I.; Hauback, B.C.; Klassen, T.; Dornheim, M. Synchrotron Diffraction Studies of Hydrogen Absorption/Desorption on CaH$_2$ + MgB$_2$ Reactive Hydride Composite Mixed With Fluorinated Compounds. *J. Phys. Chem. C* **2015**, *119*, 11430–11437. [CrossRef]

60. Dematteis, E.M.; Jensen, S.R.; Jensen, T.R.; Baricco, M. Heat capacity and thermodynamic properties of alkali and alkali-earth borohydrides. *J. Chem. Thermodyn.* **2020**, *143*, 106055. [CrossRef]

61. Tomkinson, J.; Waddington, T.C. Inelastic Neutron Scattering from the Alkali Metal Borohydrides and Calcium Borohydride. *J. Chem. Soc. Faraday Trans. 2* **1976**, *72*, 528–538. [CrossRef]

62. Dick, M.J.; Sheridan, P.M.; Wang, J.G.; Bernath, P.F. High resolution laser excitation spectroscopy of the B^{2}E-X^{2}A$_1$ transitions of calcium and strontium monoborohydride. *J. Chem. Phys.* **2007**, *126*, 164311. [CrossRef]

63. Fichtner, M.; Chlopek, K.; Longhini, M.; Hagemann, H. Vibrational spectra of Ca(BH$_4$)$_2$. *J. Phys. Chem. C* **2008**, *112*, 11575–11579. [CrossRef]

64. Reed, D.; Book, D. Recent applications of Raman spectroscopy to the study of complex hydrides for hydrogen storage. *Curr. Opin. Solid State Mater. Sci.* **2011**, *15*, 62–72. [CrossRef]

65. Kumar, S.; Nakajima, K.; Singh, A.; Kojima, Y.; Dey, G.K. Assessment of hydrogen storage property of Ca-Mg-B-H system using NMR and thermal analysis techniques. *Int. J. Hydrogen Energy* **2017**, *42*, 26007–26012. [CrossRef]

66. Hwang, S.J.; Bowman, R.C.; Reiter, J.W.; Rijssenbeek, J.; Soloveichik, G.L.; Zhao, J.C.; Kabbour, H.; Ahn, C.C. NMR confirmation for formation of [B$_{12}$H$_{12}$]$^{2-}$ complexes during hydrogen desorption from metal borohydrides. *J. Phys. Chem. C* **2008**, *112*, 3164–3169. [CrossRef]

67. Kim, C. Symmetrized Normal Mode Analysis of the Spin-Lattice Relaxation in Solid Calcium Borohydride. *Bull. Korean Chem. Soc.* **2021**, *42*, 792–797. [CrossRef]

68. Lee, H.S.; Hwang, S.J.; Kim, H.K.; Lee, Y.S.; Park, J.; Yu, J.S.; Cho, Y.W. In Situ NMR Study on the Interaction between LiBH$_4$-Ca(BH$_4$)$_2$ and Mesoporous Scaffolds. *J. Phys. Chem. Lett.* **2012**, *3*, 2922–2927. [CrossRef]

69. Frankcombe, T.J. A comment on "Prediction of crystal structure, lattice dynamical, and mechanical properties of CaB$_2$H$_2$" by Vajeeston et al., Int. J. Hydrogen Energy 36 (2011) 10149–10158. *Int. J. Hydrogen Energy* **2012**, *37*, 2709–2710. [CrossRef]

70. Han, C.L.; Dong, Y.Y.; Wang, B.Q.; Zhang, C.Y. [Ca(BH$_4$)$_2$]$_n$ Clusters as Hydrogen Storage Material: A DFT Study. *Russ. J. Phys. Chem. A* **2016**, *90*, 1997–2005. [CrossRef]

71. Hattrick-Simpers, J.R.; Hurst, W.S.; Srinivasan, S.S.; Maslar, J.E. Optical cell for combinatorial in situ Raman spectroscopic measurements of hydrogen storage materials at high pressures and temperatures. *Rev. Sci. Instrum.* **2011**, *82*, 033103. [CrossRef] [PubMed]

72. Miwa, K.; Aoki, M.; Noritake, T.; Ohba, N.; Nakamori, Y.; Towata, S.; Zuttel, A.; Orimo, S. Thermodynamical stability of calcium borohydride Ca(BH$_4$)$_2$. *Phys. Rev. B* **2006**, *74*, 155122. [CrossRef]

73. Nakamori, Y.; Li, H.W.; Kikuchi, K.; Aoki, M.; Miwa, K.; Towata, S.; Orimo, S. Thermodynamical stabilities of metal-borohydrides. *J. Alloys Compd.* **2007**, *446*, 296–300. [CrossRef]

74. Palade, P.; Comanescu, C.; Radu, C. Synthesis of Nickel and Cobalt Ferrite-Doped Graphene as Efficient Catalysts for Improving the Hydrogen Storage Kinetics of Lithium Borohydride. *Materials* **2023**, *16*, 427. [CrossRef] [PubMed]

75. Zhang, Y.S.; Majzoub, E.; Ozolins, V.; Wolverton, C. Theoretical prediction of different decomposition paths for $Ca(BH_4)_2$ and $Mg(BH_4)_2$. *Phys. Rev. B* **2010**, *82*, 174107. [CrossRef]

76. Kim, K.C.; Kulkarni, A.D.; Johnson, J.K.; Sholl, D.S. Examining the robustness of first-principles calculations for metal hydride reaction thermodynamics by detection of metastable reaction pathways. *Phys. Chem. Chem. Phys.* **2011**, *13*, 21520–21529. [CrossRef]

77. Emdadi, A.; Demir, S.; Kislak, Y.; Tekin, A. Computational Screening of Dual-Cation Metal Ammine Borohydrides by Density Functional Theory. *J. Phys. Chem. C* **2016**, *120*, 13340–13350. [CrossRef]

78. Gu, J.; Gao, M.X.; Wen, L.J.; Huang, J.J.; Liu, Y.F.; Pan, H.G. Improved hydrogen storage properties of combined $Ca(BH_4)_2$ and $LiBH_4$ system motivated by addition of $LaMg_3$ assisted with ball milling in H_2. *Int. J. Hydrogen Energy* **2015**, *40*, 12325–12335. [CrossRef]

79. Guo, Y.J.; Jia, J.F.; Wang, X.H.; Ren, Y.; Wu, H.S. Prediction of thermodynamically reversible hydrogen storage reactions in the $KBH_4/M(M = Li, Na, Ca)(BH_4)_n$(n=1,2) system from first-principles calculation. *Chem. Phys.* **2013**, *418*, 22–27. [CrossRef]

80. Guo, Y.J.; Ren, Y.; Wu, H.S.; Jia, J.F. Prediction of thermodynamically reversible hydrogen storage reactions utilizing Ca-M(M = Li, Na, K)-B-H systems: A first-principles study. *J. Mol. Model.* **2013**, *19*, 5135–5142. [CrossRef]

81. Kulkarni, A.D.; Wang, L.L.; Johnson, D.D.; Sholl, D.S.; Johnson, J.K. First-Principles Characterization of Amorphous Phases of $MB_{12}H_{12}$, M = Mg, Ca. *J. Phys. Chem. C* **2010**, *114*, 14601–14605. [CrossRef]

82. Huang, H.M.; Luo, S.J.; Xiong, Y.C. First principles investigations on the electronic properties of Cr doped α-$Ca(BH_4)_2$. *Chin. J. Phys.* **2017**, *55*, 870–875. [CrossRef]

83. Lee, S.H.; Manga, V.R.; Liu, Z.K. Effect of Mg, Ca, and Zn on stability of $LiBH_4$ through computational thermodynamics. *Int. J. Hydrogen Energy* **2010**, *35*, 6812–6821. [CrossRef]

84. Liepinya, D.; Smeu, M. A Computational Comparison of Ether and Ester Electrolyte Stability on a Ca Metal Anode. *Energy Mater. Adv.* **2021**, *2021*, 9769347. [CrossRef]

85. Mikhailin, A.A.; Charkin, D.O.; Klimenko, N.M.; Charkin, O.P. Theoretical study of elementary reactions of dehydrogenation of magnesium, calcium, zinc, and beryllium amminoborate and amminoalanate complexes. *Russ. J. Inorg. Chem.* **2013**, *58*, 416–426. [CrossRef]

86. Zhang, G.Q.; Yang, J.Z.; Fu, H.; Zheng, J.; Li, Y.; Li, X.G. Structural and electronic properties of the hydrogen storage compound $Ca(BH_4)_2$ $2NH_3$ from first-principles. *Comput. Mater. Sci.* **2012**, *54*, 345–349. [CrossRef]

87. Siegel, D.J.; Wolverton, C.; Ozolins, V. Thermodynamic guidelines for the prediction of hydrogen storage reactions and their application to destabilized hydride mixtures. *Phys. Rev. B* **2007**, *76*, 134102. [CrossRef]

88. Vajeeston, P.; Ravindran, P.; Fjellvåg, H. A new series of high hydrogen content hydrogen-storage materials—A theoretical prediction. *J. Alloys Compd.* **2007**, *446*, 44–47. [CrossRef]

89. Vajeeston, P.; Ravindran, P.; Fjellvag, H. Reply to "A comment on 'Prediction of crystal structure, lattice dynamical, and mechanical properties of CaB_2H_2' by Vajeeston et al., Int J Hydrogen Energy 36 (2011) 10149–10158" Discussion. *Int. J. Hydrogen Energy* **2012**, *37*, 2711–2712. [CrossRef]

90. Cai, W.T.; Hou, J.M.; Huang, S.Y.; Chen, J.N.; Yang, Y.Z.; Tao, P.J.; Ouyang, L.Z.; Wang, H.; Yang, X.S. Altering the chemical state of boron towards the facile synthesis of $LiBH_4$ via hydrogenating lithium compound-metal boride mixture. *Renew. Energy* **2019**, *134*, 235–240. [CrossRef]

91. Castilla-Martinez, C.A.; Moury, R.; Ould-Amara, S.; Demirci, U.B. Destabilization of Boron-Based Compounds for Hydrogen Storage in the Solid-State: Recent Advances. *Energies* **2021**, *14*, 7003. [CrossRef]

92. Durojaiye, T.; Ibikunle, A.; Goudy, A.J. Hydrogen storage in destabilized borohydride materials. *Int. J. Hydrogen Energy* **2010**, *35*, 10329–10333. [CrossRef]

93. Huang, J.J.; Gao, M.X.; Li, Z.L.; Cheng, X.B.; Gu, J.; Liu, Y.F.; Pan, H.G. Destabilization of combined $Ca(BH_4)_2$ and $Mg(AlH_4)_2$ for improved hydrogen storage properties. *J. Alloys Compd.* **2016**, *670*, 135–143. [CrossRef]

94. Ibikunle, A.A.; Goudy, A.J. Kinetics and modeling study of a $Mg(BH_4)_2/Ca(BH_4)_2$ destabilized system. *Int. J. Hydrogen Energy* **2012**, *37*, 12420–12424. [CrossRef]

95. Ibikunle, A.A.; Sabitu, S.T.; Goudy, A.J. Kinetics and modeling studies of the $CaH_2/LiBH_4$, $MgH_2/LiBH_4$, $Ca(BH_4)_2$ and $Mg(BH_4)_2$ systems. *J. Alloys Compd.* **2013**, *556*, 45–50. [CrossRef]

96. Lai, Q.W.; Aguey-Zinsou, K.F. Destabilisation of $Ca(BH_4)_2$ and $Mg(BH_4)_2$ via confinement in nanoporous Cu_2S hollow spheres. *Sustain. Energy Fuels* **2017**, *1*, 1308–1319. [CrossRef]

97. Mao, J.F.; Guo, Z.P.; Yu, X.B.; Liu, H.K. Improved Hydrogen Storage Properties of $NaBH_4$ Destabilized by CaH_2 and $Ca(BH_4)_2$. *J. Phys. Chem. C* **2011**, *115*, 9283–9290. [CrossRef]

98. Poonyayant, N.; Stavila, V.; Majzoub, E.H.; Klebanoff, L.E.; Behrens, R.; Angboonpong, N.; Ulutagay-Kartin, M.; Pakawatpanurut, P.; Hecht, E.S.; Breit, J.S. An Investigation into the Hydrogen Storage Characteristics of $Ca(BH_4)_2/LiNH_2$ and $Ca(BH_4)_2/NaNH_2$: Evidence of Intramolecular Destabilization. *J. Phys. Chem. C* **2014**, *118*, 14759–14769. [CrossRef]

99. Kim, J.H.; Jin, S.A.; Shim, J.H.; Cho, Y.W. Thermal decomposition behavior of calcium borohydride $Ca(BH_4)_2$. *J. Alloys Compd.* **2008**, *461*, L20–L22. [CrossRef]

100. Kim, Y.; Hwang, S.J.; Lee, Y.S.; Suh, J.Y.; Han, H.N.; Cho, Y.W. Hydrogen Back-Pressure Effects on the Dehydrogenation Reactions of Ca(BH$_4$)$_2$. *J. Phys. Chem. C* **2012**, *116*, 25715–25720. [CrossRef]

101. Mao, J.F.; Guo, Z.P.; Poh, C.K.; Ranjbar, A.; Guo, Y.H.; Yu, X.B.; Liu, H.K. Study on the dehydrogenation kinetics and thermodynamics of Ca(BH$_4$)$_2$. *J. Alloys Compd.* **2010**, *500*, 200–205. [CrossRef]

102. Riktor, M.D.; Sorby, M.H.; Chlopek, K.; Fichtner, M.; Hauback, B.C. The identification of a hitherto unknown intermediate phase CaB$_2$H$_x$ from decomposition of Ca(BH$_4$)$_2$. *J. Mater. Chem.* **2009**, *19*, 2754–2759. [CrossRef]

103. Lai, Q.W.; Milanese, C.; Aguey-Zinsou, K.F. Stabilization of Nanosized Borohydrides for Hydrogen Storage: Suppressing the Melting with TiCl$_3$ Doping. *ACS Appl. Energy Mater.* **2018**, *1*, 421–430. [CrossRef]

104. Yan, Y.; Rentsch, D.; Remhof, A. Controllable decomposition of Ca(BH$_4$)$_2$ for reversible hydrogen storage. *Phys. Chem. Chem. Phys.* **2017**, *19*, 7788–7792. [CrossRef] [PubMed]

105. Aoki, M.; Miwa, K.; Noritake, T.; Ohba, N.; Matsumoto, M.; Li, H.W.; Nakamori, Y.; Towata, S.; Orimo, S. Structural and dehydriding properties of Ca(BH$_4$)$_2$. *Appl. Phys. A* **2008**, *92*, 601–605. [CrossRef]

106. George, L.; Drozd, V.; Saxena, S.K.; Bardaji, E.G.; Fichtner, M. High-Pressure Investigation on Calcium Borohydride. *J. Phys. Chem. C* **2009**, *113*, 15087–15090. [CrossRef]

107. Kim, Y.; Reed, D.; Lee, Y.S.; Lee, J.Y.; Shim, J.H.; Book, D.; Cho, Y.W. Identification of the Dehydrogenated Product of Ca(BH$_4$)$_2$. *J. Phys. Chem. C* **2009**, *113*, 5865–5871. [CrossRef]

108. Sahle, C.J.; Sternemann, C.; Giacobbe, C.; Yan, Y.G.; Weis, C.; Harder, M.; Forov, Y.; Spiekermann, G.; Tolan, M.; Krisch, M.; et al. Formation of CaB$_6$ in the thermal decomposition of the hydrogen storage material Ca(BH$_4$)$_2$. *Phys. Chem. Chem. Phys.* **2016**, *18*, 19866–19872. [CrossRef]

109. Ampoumogli, A.; Charalambopoulou, G.; Javadian, P.; Richter, B.; Jensen, T.R.; Steriotis, T. Hydrogen desorption and cycling properties of composites based on mesoporous carbons and a LiBH$_4$-Ca(BH$_4$)$_2$ eutectic mixture. *J. Alloys Compd.* **2015**, *645*, S480–S484. [CrossRef]

110. Ampoumogli, A.; Steriotis, T.; Trikalitis, P.; Bardaji, E.G.; Fichtner, M.; Stubos, A.; Charalambopoulou, G. Synthesis and characterisation of a mesoporous carbon/calcium borohydride nanocomposite for hydrogen storage. *Int. J. Hydrogen Energy* **2012**, *37*, 16631–16635. [CrossRef]

111. Comanescu, C.; Capurso, G.; Maddalena, A. Nanoconfinement in activated mesoporous carbon of calcium borohydride for improved reversible hydrogen storage. *Nanotechnology* **2012**, *23*, 385401. [CrossRef] [PubMed]

112. Gu, J.; Gao, M.X.; Pan, H.G.; Liu, Y.F.; Li, B.; Yang, Y.J.; Liang, C.; Fu, H.L.; Guo, Z.X. Improved hydrogen storage performance of Ca(BH$_4$)$_2$: A synergetic effect of porous morphology and in situ formed TiO$_2$. *Eneryg Environ. Sci.* **2013**, *6*, 847–858. [CrossRef]

113. Hwang, S.J.; Lee, H.S.; To, M.; Lee, Y.S.; Cho, Y.W.; Choi, H.; Kim, C. Probing molecular dynamics of metal borohydrides on the surface of mesoporous scaffolds by multinuclear high resolution solid state NMR. *J. Alloys Compd.* **2015**, *645*, S316–S319. [CrossRef]

114. Javadian, P.; Sheppard, D.A.; Buckley, C.E.; Jensen, T.R. Hydrogen storage properties of nanoconfined LiBH$_4$-Ca(BH$_4$)$_2$. *Nano Energy* **2015**, *11*, 96–103. [CrossRef]

115. Lee, H.S.; Hwang, S.J.; To, M.; Lee, Y.S.; Cho, Y.W. Discovery of Fluidic LiBH$_4$ on Scaffold Surfaces and Its Application for Fast Co-confinement of LiBH$_4$-Ca(BH$_4$)$_2$ into Mesopores. *J. Phys. Chem. C* **2015**, *119*, 9025–9035. [CrossRef]

116. Lee, H.S.; Lee, Y.S.; Suh, J.Y.; Kim, M.; Yu, J.S.; Cho, Y.W. Enhanced Desorption and Absorption Properties of Eutectic LiBH$_4$-Ca(BH$_4$)$_2$ Infiltrated into Mesoporous Carbon. *J. Phys. Chem. C* **2011**, *115*, 20027–20035. [CrossRef]

117. Nale, A.; Pendolino, F.; Maddalena, A.; Colombo, P. Enhanced hydrogen release of metal borohydrides M(BH$_4$)$_n$ (M = Li, Na, Mg, Ca) mixed with reduced graphene oxide. *Int. J. Hydrogen Energy* **2016**, *41*, 11225–11231. [CrossRef]

118. Zhai, B.; Xiao, X.; Lin, W.; Huang, X.; Fan, X.; Li, S.; Ge, H.; Wang, Q.; Chen, L. Enhanced hydrogen desorption properties of LiBH$_4$-Ca(BH$_4$)$_2$ by a synergetic effect of nanoconfinement and catalysis. *Int. J. Hydrogen Energy* **2016**, *41*, 17462–17470. [CrossRef]

119. Barkhordarian, G.; Klassen, T.; Dornheim, M.; Bormann, R. Unexpected kinetic effect of MgB$_2$ in reactive hydride composites containing complex borohydrides. *J. Alloys Compd.* **2007**, *440*, L18–L21. [CrossRef]

120. Boynuegri, T.A.; Guru, M. Catalytic dehydrogenation of calcium borohydride by using hydrogel catalyst. *Int. J. Hydrogen Energy* **2017**, *42*, 17869–17873. [CrossRef]

121. Boynuegri, T.A.; Karabulut, A.F.; Guru, M. Synthesis of Borohydride and Catalytic Dehydrogenation by Hydrogel Based Catalyst. *J. Electron. Mater.* **2016**, *45*, 3949–3956. [CrossRef]

122. Chu, H.L.; Qiu, S.J.; Liu, L.; Zou, Y.J.; Xiang, C.L.; Zhang, H.Z.; Xu, F.; Sun, L.X.; Zhou, H.Y.; Wu, G.T. Significantly enhanced dehydrogenation properties of calcium borohydride combined with urea. *Dalton Trans.* **2014**, *43*, 15291–15294. [CrossRef]

123. Chu, H.L.; Qiu, S.; Sun, L.; Wu, G. Improved hydrogen desorption properties of Li-Ca-B-N-H system catalyzed by cobalt containing species. *J. Renew. Sustain. Energy* **2014**, *6*, 013105. [CrossRef]

124. Chu, H.L.; Qiu, S.J.; Zou, Y.J.; Xiang, C.L.; Zhang, H.Z.; Xu, F.; Sun, L.X.; Zhou, H.Y. Improvement on Hydrogen Desorption Performance of Calcium Borohydride Diammoniate Doped with Transition Metal Chlorides. *J. Phys. Chem. C* **2015**, *119*, 913–918. [CrossRef]

125. Gosalawit-Utke, R.; Suarez, K.; Von Colbe, J.M.B.; Bösenberg, U.; Jensen, T.R.; Cerenius, Y.; Minella, C.B.; Pistidda, C.; Barkhordarian, G.; Schulze, M.; et al. Ca(BH$_4$)$_2$-MgF$_2$ reversible hydrogen storage: Reaction mechanisms and kinetic properties. *J. Phys. Chem. C* **2011**, *115*, 3762–3768. [CrossRef]

126. Jansa, I.L.; Friedrichs, O.; Fichtner, M.; Bardají, E.G.; Züttel, A.; Hauback, B.C. Effects of Ball Milling and TiF$_3$ Addition on the Dehydrogenation Temperature of Ca(BH$_4$)$_2$ Polymorphs. *Energies* **2020**, *13*, 4828. [CrossRef]

127. Karimi, F.; Pranzas, P.K.; Pistidda, C.; Puszkiel, J.A.; Milanese, C.; Vainio, U.; Paskevicius, M.; Emmler, T.; Santoru, A.; Utke, R.; et al. Structural and kinetic investigation of the hydride composite Ca(BH$_4$)$_2$ + MgH$_2$ system doped with NbF$_5$ for solid-state hydrogen storage. *Phys. Chem. Chem. Phys.* **2015**, *17*, 27328–27342. [CrossRef]

128. Wang, Z.G.; Hui, Q.; Wang, C.L.; Cheng, N.P. First-principle study of the effects of Nb and Ti doping on the dehydrogenation properties of Ca(BH$_4$)$_2$. *Comput. Mater. Sci.* **2011**, *50*, 3114–3118. [CrossRef]

129. Kim, D.H.; Jo, S.; Kwon, J.; Lee, S.; Eom, K. Effect of iron content on the hydrogen production kinetics of electroless-deposited Co-Ni-Fe-P alloy catalysts from the hydrolysis of sodium borohydride, and a study of its feasibility in a new hydrolysis using magnesium and calcium borohydrides. *Int. J. Hydrogen Energy* **2019**, *44*, 15228–15238. [CrossRef]

130. Lee, J.Y.; Lee, Y.S.; Suh, J.Y.; Shim, J.H.; Cho, Y.W. Metal halide doped metal borohydrides for hydrogen storage: The case of Ca(BH$_4$)$_2$-CaX$_2$ (X = F, Cl) mixture. *J. Alloys Compd.* **2010**, *506*, 721–727. [CrossRef]

131. Li, B.; Liu, Y.F.; Gu, J.; Gao, M.X.; Pan, H.G. Synergetic Effects of In Situ Formed CaH$_2$ and LiBH$_4$ on Hydrogen Storage Properties of the Li-Mg-N-H System. *Chem.-Asian J.* **2013**, *8*, 374–384. [CrossRef] [PubMed]

132. Minella, C.B.; Garroni, S.; Pistidda, C.; Baro, M.D.; Gutfleisch, O.; Klassen, T.; Dornheim, M. Sorption properties and reversibility of Ti(IV) and Nb(V)-fluoride doped—Ca(BH$_4$)$_2$-MgH$_2$ system. *J. Alloys Compd.* **2015**, *622*, 989–994. [CrossRef]

133. Minella, C.B.; Garroni, S.; Pistidda, C.; Gosalawit-Utke, R.; Barkhordarian, G.; Rongeat, C.; Lindemann, I.; Gutfleisch, O.; Jensen, T.R.; Cerenius, Y.; et al. Effect of Transition Metal Fluorides on the Sorption Properties and Reversible Formation of Ca(BH$_4$)$_2$. *J. Phys. Chem. C* **2011**, *115*, 2497–2504. [CrossRef]

134. Minella, C.B.; Pellicer, E.; Rossinyol, E.; Karimi, F.; Pistidda, C.; Garroni, S.; Milanese, C.; Nolis, P.; Baro, M.D.; Gutfleisch, O.; et al. Chemical State, Distribution, and Role of Ti- and Nb-Based Additives on the Ca(BH$_4$)$_2$ System. *J. Phys. Chem. C* **2013**, *117*, 4394–4403. [CrossRef]

135. Mustafa, N.S.; Ismail, M. Significant effect of TiF$_3$ on the performance of 2NaAlH$_4$+Ca(BH$_4$)$_2$ hydrogen storage properties. *Int. J. Hydrogen Energy* **2019**, *44*, 21979–21987. [CrossRef]

136. Pendolino, F. "Boron Effect" on the Thermal Decomposition of Light Metal Borohydrides MBH$_4$ (M = Li, Na, Ca). *J. Phys. Chem. C* **2012**, *116*, 1390–1394. [CrossRef]

137. Pistidda, C.; Karimi, F.; Garroni, S.; Rzeszutek, A.; Minella, C.B.; Milanese, C.; Le, T.T.; Rude, L.H.; Skibsted, J.; Jensen, T.R.; et al. Effect of the Partial Replacement of CaH$_2$ with CaF$_2$ in the Mixed System CaH$_2$ + MgB$_2$. *J. Phys. Chem. C* **2014**, *118*, 28409–28417. [CrossRef]

138. Rongeat, C.; D'Anna, V.; Hagemann, H.; Borgschulte, A.; Zuttel, A.; Schultz, L.; Gutfleisch, O. Effect of additives on the synthesis and reversibility of Ca(BH$_4$)$_2$. *J. Alloys Compd.* **2010**, *493*, 281–287. [CrossRef]

139. Schiavo, B.; Girella, A.; Agresti, F.; Capurso, G.; Milanese, C. Ball-milling and AlB$_2$ addition effects on the hydrogen sorption properties of the CaH$_2$ + MgB$_2$ system. *J. Alloys Compd.* **2011**, *509*, S714–S718. [CrossRef]

140. Amama, P.B.; Spowart, J.E.; Voevodin, A.A.; Fisher, T.S. Modified Magnesium Hydride and Calcium Borohydride for High-Capacity Thermal Energy Storage. In Proceedings of the 8th ASME/JSME Thermal Engineering Joint Conference, Honolulu, HI, USA, 13–17 March 2011; American Society of Mechanical Engineers: Honolulu, HI, USA, 2011; pp. 1617–1623. [CrossRef]

141. Minella, C.B.; Garroni, S.; Olid, D.; Teixidor, F.; Pistidda, C.; Lindemann, I.; Gutfleisch, O.; Baro, M.D.; Bormann, R.; Klassen, T.; et al. Experimental Evidence of Ca[B$_{12}$H$_{12}$] Formation During Decomposition of a Ca(BH$_4$)$_2$ + MgH$_2$ Based Reactive Hydride Composite. *J. Phys. Chem. C* **2011**, *115*, 18010–18014. [CrossRef]

142. Minella, C.B.; Pistidda, C.; Garroni, S.; Nolis, P.; Baro, M.D.; Gutfleisch, O.; Klassen, T.; Bormann, R.; Dornheim, M. Ca(BH$_4$)$_2$ + MgH$_2$: Desorption Reaction and Role of Mg on Its Reversibility. *J. Phys. Chem. C* **2013**, *117*, 3846–3852. [CrossRef]

143. Pinkerton, F.E.; Meyer, M.S. Reversible hydrogen storage in the lithium borohydride—Calcium hydride coupled system. *J. Alloys Compd.* **2008**, *464*, L1–L4. [CrossRef]

144. Li, Y.; Li, P.; Qu, X.H. Investigation on LiBH$_4$-CaH$_2$ composite and its potential for thermal energy storage. *Sci. Rep.* **2017**, *7*, srep41754. [CrossRef] [PubMed]

145. Qiu, S.J.; Chu, H.L.; Zou, Y.J.; Xiang, C.L.; Xu, F.; Sun, L.X. Light metal borohydrides/amides combined hydrogen storage systems: Composition, structure and properties. *J. Mater. Chem. A* **2017**, *5*, 25112–25130. [CrossRef]

146. Yu, X.B.; Yang, Z.X.; Guo, Y.H.; Li, S.G. Thermal decomposition performance of Ca(BH$_4$)$_2$/LiNH$_2$ mixtures. *J. Alloys Compd.* **2011**, *509*, S724–S727. [CrossRef]

147. Chu, H.; Xiong, Z.; Wu, G.; Guo, J.; Zheng, X.; He, T.; Wu, C.; Chen, P. Hydrogen storage properties of Ca(BH$_4$)$_2$-LiNH$_2$ system. *Chem. Asian J.* **2010**, *5*, 1594–1599. [CrossRef]

148. Morelle, F.; Jepsen, L.H.; Jensen, T.R.; Sharma, M.; Hagemann, H.; Filinchuk, Y. Reaction Pathways in Ca(BH$_4$)$_2$-NaNH$_2$ and Mg(BH$_4$)$_2$-NaNH$_2$ Hydrogen-Rich Systems. *J. Phys. Chem. C* **2016**, *120*, 8428–8435. [CrossRef]

149. Chu, H.L.; Xiong, Z.; Wu, G.; Guo, J.; He, T.; Chen, P. Improved dehydrogenation properties of Ca(BH$_4$)$_2$-LiNH$_2$ combined system. *Dalton Trans.* **2010**, *39*, 10585–10587. [CrossRef]

150. Roedern, E.; Jensen, T.R. Thermal Decomposition of Mn(BH$_4$)$_2$-M(BH$_4$)$_x$ and Mn(BH$_4$)$_2$-MH$_x$ Composites with M = Li, Na, Mg, and Ca. *J. Phys. Chem. C* **2014**, *118*, 23567–23574. [CrossRef]

151. Bergemann, N.; Pistidda, C.; Milanese, C.; Aramini, M.; Huotari, S.; Nolis, P.; Santoru, A.; Chierotti, M.R.; Chaudhary, A.L.; Baro, M.D.; et al. A hydride composite featuring mutual destabilisation and reversible boron exchange: $Ca(BH_4)_2$-Mg_2NiH_4. *J. Mater. Chem. A* **2018**, *6*, 17929–17946. [CrossRef]

152. Chu, H.L.; Wu, G.T.; Zhang, Y.; Xiong, Z.T.; Guo, J.P.; He, T.; Chen, P. Improved Dehydrogenation Properties of Calcium Borohydride Combined with Alkaline-Earth Metal Amides. *J. Phys. Chem. C* **2011**, *115*, 18035–18041. [CrossRef]

153. Dematteis, E.M.; Baricco, M. Hydrogen Desorption in $Mg(BH_4)_2$-$Ca(BH_4)_2$ System. *Energies* **2019**, *12*, 3230. [CrossRef]

154. Dematteis, E.M.; Pistidda, C.; Dornheim, M.; Baricco, M. Exploring Ternary and Quaternary Mixtures in the $LiBH_4$-$NaBH_4$-KBH_4-$Mg(BH_4)_2$-$Ca(BH_4)_2$ System. *Chemphyschem* **2019**, *20*, 1348–1359. [CrossRef] [PubMed]

155. Dematteis, E.M.; Santoru, A.; Poletti, M.G.; Pistidda, C.; Klassen, T.; Dornheim, M.; Baricco, M. Phase stability and hydrogen desorption in a quinary equimolar mixture of light-metals borohydrides. *Int. J. Hydrogen Energy* **2018**, *43*, 16793–16803. [CrossRef]

156. Javadian, P.; GharibDoust, S.P.; Li, H.W.; Sheppard, D.A.; Buckley, C.E.; Jensen, T.R. Reversibility of $LiBH_4$ Facilitated by the $LiBH_4$-$Ca(BH_4)_2$ Eutectic. *J. Phys. Chem. C* **2017**, *121*, 18439–18449. [CrossRef]

157. Paskevicius, M.; Ley, M.B.; Sheppard, D.A.; Jensen, T.R.; Buckley, C.E. Eutectic melting in metal borohydrides. *Phys. Chem. Chem. Phys.* **2013**, *15*, 19774–19789. [CrossRef] [PubMed]

158. Li, B.; Liu, Y.F.; Gu, J.; Gu, Y.J.; Gao, M.X.; Pan, H.G. Mechanistic investigations on significantly improved hydrogen storage performance of the $Ca(BH_4)_2$-added $2LiNH_2/MgH_2$ system. *Int. J. Hydrogen Energy* **2013**, *38*, 5030–5038. [CrossRef]

159. Meggouh, M.; Grant, D.M.; Deavin, O.; Brunelli, M.; Hansen, T.C.; Walker, G.S. Investigation of the dehydrogenation behavior of the $2LiBH_4$:$CaNi_5$ multicomponent hydride system. *Int. J. Hydrogen Energy* **2015**, *40*, 2989–2996. [CrossRef]

160. Moller, K.T.; Grinderslev, J.B.; Jensen, T.R. A $NaAlH_4$-$Ca(BH_4)_2$ composite system for hydrogen storage. *J. Alloys Compd.* **2017**, *720*, 497–501. [CrossRef]

161. Mustafa, N.S.; Yap, F.A.H.; Yahya, M.S.; Ismail, M. The hydrogen storage properties and reaction mechanism of the $NaAlH_4$ + $Ca(BH_4)_2$ composite system. *Int. J. Hydrogen Energy* **2018**, *43*, 11132–11140. [CrossRef]

162. Gao, M.; Gu, J.; Pan, H.; Wang, Y.; Liu, Y.; Liang, C.; Guo, Z. $Ca(BH_4)_2$-$LiBH_4$-MgH_2: A novel ternary hydrogen storage system with superior long-term cycling performance. *J. Mater. Chem. A* **2013**, *1*, 12285–12292. [CrossRef]

163. Gonzalez-Silveira, M.; Gremaud, R.; Schreuders, H.; van Setten, M.J.; Batyrev, E.; Rougier, A.; Dupont, L.; Bardaji, E.G.; Lohstroh, W.; Dam, B. In-Situ Deposition of Alkali and Alkaline Earth Hydride Thin Films To Investigate the Formation of Reactive Hydride Composites. *J. Phys. Chem. C* **2010**, *114*, 13895–13901. [CrossRef]

164. Grube, E.; Jensen, S.R.H.; Nielsen, U.G.; Jensen, T.R. Reactivity of magnesium borohydride—Metal hydride composites, gamma-$Mg(BH_4)_2$-MHx, M = Li, Na, Mg, Ca. *J. Alloys Compd.* **2019**, *770*, 1155–1163. [CrossRef]

165. Kim, J.M.; Kim, Y.; Shim, J.H.; Lee, Y.S.; Suh, J.Y.; Ahn, J.P.; Kim, G.H.; Cho, Y.W. Microstructural Analysis of Dehydrogenation Products of the $Ca(BH_4)_2$-MgH_2 Composite. *Microsc. Microanal.* **2013**, *19*, 149–151. [CrossRef] [PubMed]

166. Lee, J.Y.; Ravnsbaek, D.; Lee, Y.S.; Kim, Y.; Cerenius, Y.; Shim, J.H.; Jensen, T.R.; Hur, N.H.; Cho, Y.W. Decomposition Reactions and Reversibility of the $LiBH_4$-$Ca(BH_4)_2$ Composite. *J. Phys. Chem. C* **2009**, *113*, 15080–15086. [CrossRef]

167. Yan, Y.G.; Remhof, A.; Mauron, P.; Rentsch, D.; Lodziana, Z.; Lee, Y.S.; Lee, H.S.; Cho, Y.W.; Zuttel, A. Controlling the Dehydrogenation Reaction toward Reversibility of the $LiBH_4$-$Ca(BH_4)_2$ Eutectic System. *J. Phys. Chem. C* **2013**, *117*, 8878–8886. [CrossRef]

168. Ley, M.B.; Roedern, E.; Thygesen, P.M.M.; Jensen, T.R. Melting Behavior and Thermolysis of $NaBH_4$-$Mg(BH_4)_2$ and $NaBH_4$-$Ca(BH_4)_2$ Composites. *Energies* **2015**, *8*, 2701–2713. [CrossRef]

169. Tang, Z.W.; Guo, Y.H.; Li, S.F.; Yu, X.B. Low-Temperature Hydrogen Generation and Ammonia Suppression from Calcium Borohydride Combined with Guanidinium Borohydride. *J. Phys. Chem. C* **2011**, *115*, 3188–3193. [CrossRef]

170. Alcantara, K.S.; Boesenberg, U.; Zavorotynska, O.; von Colbe, J.B.; Taube, K.; Baricco, M.; Klassen, T.; Dornheim, M. Sorption and desorption properties of a $CaH_2/MgB_2/CaF_2$ reactive hydride composite as potential hydrogen storage material. *J. Solid State Chem.* **2011**, *184*, 3104–3109. [CrossRef]

171. Alcantara, K.S.; Ramallo-Lopez, J.M.; Boesenberg, U.; Saldan, I.; Pistidda, C.; Requejo, F.G.; Jensen, T.; Cerenius, Y.; Sorby, M.; Avila, J.; et al. $3CaH_2$ + $4MgB_2$ + CaF_2 Reactive Hydride Composite as a Potential Hydrogen Storage Material: Hydrogenation and Dehydrogenation Pathway. *J. Phys. Chem. C* **2012**, *116*, 7207–7212. [CrossRef]

172. Chaudhary, A.L.; Li, G.Q.; Matsuo, M.; Orimo, S.; Deledda, S.; Sorby, M.H.; Hauback, B.C.; Pistidda, C.; Klassen, T.; Dornheim, M. Simultaneous desorption behavior of M borohydrides and Mg_2FeH_6 reactive hydride composites (M = Mg, then Li, Na, K, Ca). *Appl. Phys. Lett.* **2015**, *107*, 073905. [CrossRef]

173. Dematteis, E.M.; Vaunois, S.; Pistidda, C.; Dornheim, M.; Baricco, M. Reactive Hydride Composite of Mg_2NiH_4 with Borohydrides Eutectic Mixtures. *Crystals* **2018**, *8*, 90. [CrossRef]

174. Arumugam, S.; Angamuthu, A.; Gopalan, P. Molecular Insights on the Dihydrogen Bond Properties of Metal Borohydride Complexes upon Ammoniation. *ECS J. Solid State Sci. Technol.* **2021**, *10*, 091006. [CrossRef]

175. Kiruthika, S.; Ravindran, P. Chemical Bonding Analysis on Amphoteric Hydrogen-Alkaline Earth Ammine Borohydrides. In Proceedings of the 62nd DAE Solid State Physics Symposium, Mumbai, India, 26–30 December 2017; American Institute of Physics: Mumbai, India, 2017. [CrossRef]

176. Wang, K.; Zhang, J.G.; Jiao, J.S.; Zhang, T.L.; Zhou, Z.N. A First-Principles Study: Structure and Decomposition of Mono-/Bimetallic Ammine Borohydrides. *J. Phys. Chem. C* **2014**, *118*, 8271–8279. [CrossRef]

177. Chen, X.W.; Yu, X.B. Electronic Structure and Initial Dehydrogenation Mechanism of $M(BH_4)_2 \cdot 2NH_3$ (M = Mg, Ca, and Zn): A First-Principles Investigation. *J. Phys. Chem. C* **2012**, *116*, 11900–11906. [CrossRef]

178. Yuan, P.-F.; Wang, F.; Sun, Q.; Jia, Y.; Guo, Z.-X. Structural, energetic and thermodynamic analyses of $Ca(BH_4)_2 \cdot 2NH_3$ from first principles calculations. *J. Solid State Chem.* **2012**, *185*, 206–212. [CrossRef]

179. Chen, X.W.; Yuan, F.; Tan, Y.B.; Tang, Z.W.; Yu, X.B. Improved Dehydrogenation Properties of $Ca(BH_4)_2 \cdot nNH_3$ (n = 1, 2, and 4) Combined with $Mg(BH_4)_2$. *J. Phys. Chem. C* **2012**, *116*, 21162–21168. [CrossRef]

180. Lobkovskii, E.B.; Chekhlov, A.N.; Levicheva, M.D.; Titov, L.V. Crystalline and molecular-structure of calcium borohydride complex with dimethyl ether of diethyleneglycole-$Ca(BH_4)_2$ 2DG. *Koord. Khimiya* **1988**, *14*, 543–550.

181. Titov, L.V.; Petrovskii, P.V. Synthesis and Some Properties of Calcium Tetradecahydroundecaborate $Ca(B_{11}H_{14})_2 \cdot 4Dg$ (Dg = Diglyme). *Russ. J. Inorg. Chem.* **2011**, *56*, 1032–1033. [CrossRef]

182. Chu, H.L.; Wu, G.T.; Xiong, Z.T.; Guo, J.P.; He, T.; Chen, P. Structure and Hydrogen Storage Properties of Calcium Borohydride Diammoniate. *Chem. Mater.* **2010**, *22*, 6021–6028. [CrossRef]

183. Huang, Z.N.; Wang, Y.Q.; Zheng, L.; Wang, D.; Yang, F.S.; Wu, Z.; Wu, L.; Zhang, Z.X. Decomposition mechanisms and the role of transition metal impurities in the kinetics of $Ca(BH_4)_2 \cdot 2NH_3$. *Int. J. Hydrogen Energy* **2020**, *45*, 2999–3007. [CrossRef]

184. Tang, Z.W.; Tan, Y.B.; Gu, Q.F.; Yu, X.B. A novel aided-cation strategy to advance the dehydrogenation of calcium borohydride monoammoniate. *J. Mater. Chem.* **2012**, *22*, 5312–5318. [CrossRef]

185. Li, Z.; He, T.; Wu, G.T.; Ju, X.H.; Chen, P. The synthesis, structure and dehydrogenation of calcium borohydride hydrazinates. *Int. J. Hydrogen Energy* **2015**, *40*, 5333–5339. [CrossRef]

186. Wu, H.; Zhou, W.; Pinkerton, F.E.; Meyer, M.S.; Srinivas, G.; Yildirim, T.; Udovic, T.J.; Rush, J.J. A new family of metal borohydride ammonia borane complexes: Synthesis, structures, and hydrogen storage properties. *J. Mater. Chem.* **2010**, *20*, 6550–6556. [CrossRef]

187. Wu, H.; Zhou, X.Q.; Rodriguez, E.E.; Zhou, W.; Udovic, T.J.; Yildirim, T.; Rush, J.J. A new family of metal borohydride guanidinate complexes: Synthesis, structures and hydrogen-storage properties. *J. Solid State Chem.* **2016**, *242*, 186–192. [CrossRef]

188. Kim, Y.; Reed, D.; Lee, Y.S.; Shim, J.H.; Han, H.N.; Book, D.; Cho, Y.W. Hydrogenation reaction of CaH_2-CaB_6-Mg mixture. *J. Alloys Compd.* **2010**, *492*, 597–600. [CrossRef]

189. Li, H.W.; Akiba, E.; Orimo, S. Comparative study on the reversibility of pure metal borohydrides. *J. Alloys Compd.* **2013**, *580*, S292–S295. [CrossRef]

190. Riktor, M.D.; Sorby, M.H.; Muller, J.; Bardaji, E.G.; Fichtner, M.; Hauback, B.C. On the rehydrogenation of decomposed $Ca(BH_4)_2$. *J. Alloys Compd.* **2015**, *632*, 800–804. [CrossRef]

191. Li, Y.; Li, P.; Tan, Q.W.; Zhang, Z.L.; Wan, Q.; Liu, Z.W.; Subramanian, A.; Qu, X.H. Thermal properties and cycling performance of $Ca(BH_4)_2/MgH_2$ composite for energy storage. *Chem. Phys. Lett.* **2018**, *700*, 44–49. [CrossRef]

192. Bergemann, N.; Pistidda, C.; Milanese, C.; Emmler, T.; Karimi, F.; Chaudhary, A.L.; Chierotti, M.R.; Klassen, T.; Dornheim, M. $Ca(BH_4)_2$-Mg_2NiH_4: On the pathway to a $Ca(BH_4)_2$ system with a reversible hydrogen cycle. *Chem. Commun.* **2016**, *52*, 4836–4839. [CrossRef]

193. Kim, Y.; Hwang, S.J.; Shim, J.H.; Lee, Y.S.; Han, H.N.; Cho, Y.W. Investigation of the Dehydrogenation Reaction Pathway of $Ca(BH_4)_2$ and Reversibility of Intermediate Phases. *J. Phys. Chem. C* **2012**, *116*, 4330–4334. [CrossRef]

194. Ozolins, V.; Majzoub, E.H.; Wolverton, C. First-Principles Prediction of Thermodynamically Reversible Hydrogen Storage Reactions in the Li-Mg-Ca-B-H System. *J. Am. Chem. Soc.* **2009**, *131*, 230–237. [CrossRef] [PubMed]

195. Wang, L.L.; Graham, D.D.; Robertson, I.M.; Johnson, D.D. On the Reversibility of Hydrogen-Storage Reactions in $Ca(BH_4)_2$: Characterization via Experiment and Theory. *J. Phys. Chem. C* **2009**, *113*, 20088–20096. [CrossRef]

196. Kim, J.H.; Jin, S.A.; Shim, J.H.; Cho, Y.W. Reversible hydrogen storage in calcium borohydride $Ca(BH_4)_2$. *Scr. Mater.* **2008**, *58*, 481–483. [CrossRef]

197. Kim, J.H.; Shim, J.H.; Cho, Y.W. On the reversibility of hydrogen storage in Ti- and Nb-catalyzed $Ca(BH_4)_2$. *J. Power Sources* **2008**, *181*, 140–143. [CrossRef]

198. Liu, D.M.; Gao, C.; Qian, Z.X.; Si, T.Z.; Zhang, Q.A. Reversible hydrogen storage in $LiBH_4/Ca(AlH_4)_2$ systems. *Int. J. Hydrogen Energy* **2013**, *38*, 3291–3296. [CrossRef]

199. Yan, Y.; Remhof, A.; Rentsch, D.; Züttel, A.; Giri, S.; Jena, P. A novel strategy for reversible hydrogen storage in $Ca(BH_4)_2$. *Chem. Commun.* **2015**, *51*, 11008–11011. [CrossRef]

200. Didelot, E.; Cerny, R. Ionic conduction in bimetallic borohydride borate, $LiCa_3(BH_4)(BO_3)_2$. *Solid State Ion.* **2017**, *305*, 16–22. [CrossRef]

201. Hahn, N.T.; Self, J.; Han, K.S.; Murugesan, V.; Mueller, K.T.; Persson, K.A.; Zavadil, K.R. Quantifying Species Populations in Multivalent Borohydride Electrolytes. *J. Phys. Chem. B* **2021**, *125*, 3644–3652. [CrossRef]

202. Hahn, N.T.; Self, J.; Seguin, T.J.; Driscoll, D.M.; Rodriguez, M.A.; Balasubramanian, M.; Persson, K.A.; Zavadil, K.R. The critical role of configurational flexibility in facilitating reversible reactive metal deposition from borohydride solutions. *J. Mater. Chem. A* **2020**, *8*, 7235–7244. [CrossRef]

203. Melemed, A.M.; Skiba, D.A.; Gallant, B.M. Toggling Calcium Plating Activity and Reversibility through Modulation of Ca^{2+} Speciation in Borohydride-Based Electrolytes. *J. Phys. Chem. C* **2022**, *126*, 892–902. [CrossRef] [PubMed]

204. Mezaki, T.; Kuronuma, Y.; Oikawa, I.; Kamegawa, A.; Takamura, H. Li-Ion Conductivity and Phase Stability of Ca-Doped $LiBH_4$ under High Pressure. *Inorg Chem* **2016**, *55*, 10484–10489. [CrossRef] [PubMed]

205. Sveinbjornsson, D.; Blanchard, D.; Myrdal, J.S.G.; Younesi, R.; Viskinde, R.; Riktor, M.D.; Norby, P.; Vegge, T. Ionic conductivity and the formation of cubic CaH$_2$ in the LiBH$_4$-Ca(BH$_4$)$_2$ composite. *J. Solid State Chem.* **2014**, *211*, 81–89. [CrossRef]

206. Yang, F.; Feng, X.; Zhuo, Z.; Vallez, L.; Liu, Y.-S.; McClary, S.A.; Hahn, N.T.; Glans, P.-A.; Zavadil, K.R.; Guo, J. Ca^{2+} Solvation and Electrochemical Solid/Electrolyte Interphase Formation toward the Multivalent-Ion Batteries. *Arab. J. Sci. Eng.* **2023**, *48*, 7243–7262. [CrossRef]

207. Yang, J.; Jiao, Y.; Han, Y.-H.; Li, J. Pressure-Induced Metallization and Electrical Phase Diagram for Polycrystalline CaB$_6$ under High Pressure and Low Temperature. *Chin. Phys. Lett.* **2016**, *33*, 086201. [CrossRef]

208. Di Cataldo, S.; Boeri, L. Metal borohydrides as ambient-pressure high-*T*c superconductors. *Phys. Rev. B* **2023**, *107*, L060501. [CrossRef]

209. Yang, W.-H.; Lu, W.-C.; Qin, W.; Sun, H.-J.; Xue, X.-Y.; Ho, K.M.; Wang, C.Z. Pressure-induced superconductivity in the hydrogen-rich pseudobinary CaB-H$_n$ compounds. *Phys. Rev. B* **2021**, *104*, 174106. [CrossRef]

210. Kuzdrowska, M.; Annunziata, L.; Marks, S.; Schmid, M.; Jaffredo, C.G.; Roesky, P.W.; Guillaume, S.M.; Maron, L. Organometallic calcium and strontium borohydrides as initiators for the polymerization of epsilon-caprolactone and L-lactide: Combined experimental and computational investigations. *Dalton Trans.* **2013**, *42*, 9352–9360. [CrossRef]

211. Daugan, A.; Brown, E. Lignanes, 11. Preparation of (R)-(+)-Beta-Vanyllyl-Gamma-Butyrolactone and Its Use in Total Synthesis of Natural Lignanes. *J. Nat. Prod.* **1991**, *54*, 110–118. [CrossRef]

212. Matsui, M.; Miyano, M.; Tomita, K. Calcium Borohydride Reduction of Beta-Ketoesters. *Bull. Agric. Chem. Soc. Jpn.* **1956**, *20*, 139–140. [CrossRef]

213. Narasimhan, S.; Prasad, K.G.; Madhavan, S. Calcium Borohydride—A Reagent for Facile Conversion of Carboxylic Esters to Alcohols and Aldehydes. *Synth. Commun.* **1995**, *25*, 1689–1697. [CrossRef]

214. Narasimhan, S.; Prasad, K.G.; Madhavan, S. Remarkable Regioselective Hydroboration of Terminal Alkenes by Calcium Borohydride. *Tetrahedron Lett.* **1995**, *36*, 1141–1144. [CrossRef]

215. Narasimhan, S.; Prasad, K.G.; Prasanna, R. Alkene-catalyzed reductions of esters by calcium borohydride. *ChemInform* **1993**, *24*, 102. [CrossRef]

216. Firouzabadi, H.; Tamami, B.; Kiasat, A.R. Efficient reduction of aryl azides and aryl nitro compounds to their corresponding amines with sulfurated calcium borohydride Ca(BH$_2$S$_3$)$_2$. A new modified borohydride agent. *Synth. Commun.* **2000**, *30*, 587–596. [CrossRef]

217. Firouzabadi, H.; Tamami, B.; Kiasat, A.R. Efficient reduction of organic compounds with sulfurated calcium borohydride Ca(S$_3$BH$_2$)$_2$, a new and stable modified borohydride reagent. *Phosphorus Sulfur Silicon Relat. Elem.* **2000**, *159*, 99–108. [CrossRef]

218. Hallouis, S.; Saluzzo, C.; Amouroux, R. Grignard reagent/borohydride combinations alkylation/reduction of esters. *Synth. Commun.* **2000**, *30*, 313–324. [CrossRef]

219. Xu, W.L.; Wang, R.M.; Wu, G.T.; Chen, P. Calcium amidoborane, a new reagent for chemoselective reduction of alpha, beta-unsaturated aldehydes and ketones to allylic alcohols. *Rsc Adv.* **2012**, *2*, 6005–6010. [CrossRef]

220. Barrett, A.G.M.; Crimmin, M.R.; Hill, M.S.; Hitchcock, P.B.; Procopiou, P.A. Reactions of beta-diketiminate-stabilized calcium amides with 9-borabicyclo [3.3.1] nonane (9-BBN). *Organometallics* **2007**, *26*, 4076–4079. [CrossRef]

221. Bellham, P.; Hill, M.S.; Kociok-Kohn, G. Stoichiometric and Catalytic Reactivity of tert-Butylamine Borane with Calcium Silylamides. *Organometallics* **2014**, *33*, 5716–5721. [CrossRef]

222. Bonnet, F.; Stoffelbach, F.; Fontaine, G.; Bourbigot, S. Continuous cyclo-polymerisation of L-lactide by reactive extrusion using atoxic metal-based catalysts: Easy access to well-defined polylactide macrocycles. *RSC Adv.* **2015**, *5*, 31303–31310. [CrossRef]

223. Collins, R.A.; Unruangsri, J.; Mountford, P. Synthesis and rac-lactide ring-opening polymerisation studies of new alkaline earth tetrahydroborate complexes. *Dalton Trans.* **2013**, *42*, 759–769. [CrossRef] [PubMed]

224. Cushion, M.G.; Mountford, P. Cationic and charge-neutral calcium tetrahydroborate complexes and their use in the controlled ring-opening polymerisation of rac-lactide. *Chem. Commun.* **2011**, *47*, 2276–2278. [CrossRef] [PubMed]

225. Borisov, A.P.; Makhaev, V.D. Preparation of calcium cyclopentadienyl complexes using calcium borohydride. *Russ. Chem. Bull.* **1993**, *42*, 339–340. [CrossRef]

226. Chakrabarti, N.; Quinlivan, P.J.; Parkin, G. Synthesis and Structural Characterization of [BmMeBenz)$_2$Ca(THF)$_2$: Ca$\cdots$H-B interactions in a Sulfur-Rich Coordination Environment. *J. Mex. Chem. Soc.* **2017**, *61*, 90–96. [CrossRef]

227. Erickson, K.A.; Scott, B.L.; Kiplinger, J.L. Ca(BH$_4$)$_2$ as a simple tool for the preparation of thorium and uranium metallocene borohydride complexes: First synthesis and crystal structure of (C$_5$Me$_5$)$_2$Th(η^3-H$_3$BH)$_2$. *Inorg. Chem. Commun.* **2017**, *77*, 44–46. [CrossRef]

228. Furtat, P.; Lenz-Leite, M.; Ionescu, E.; Machado, R.A.F.; Motz, G. Synthesis of fluorine-modified polysilazanes via Si-H bond activation and their application as protective hydrophobic coatings. *J. Mater. Chem. A* **2017**, *5*, 25509–25521. [CrossRef]

229. Comanescu, C. Graphene Supports for Metal Hydride and Energy Storage Applications. *Crystals* **2023**, *13*, 878. [CrossRef]